

Consequences of Neglecting the Interannual Variability of the Solar Resource: A Case Study of Photovoltaic Power Among the Hawaiian Islands

Richard Bryce^{a,b}, Ignacio Losada Carreño^{a,c}, Andrew Kumler^a, Bri-Mathias Hodge^a, Billy Roberts^a, Carlo Brancucci Martinez-Anido^a

^a National Renewable Energy Laboratory, Golden Colorado

^b Department of Mechanical and Industrial Engineering, University of Massachusetts, Amherst Massachusetts

^c Department of Mechanical Engineering, Northern Arizona University, Flagstaff Arizona

Abstract

The interannual variability of the solar irradiance and meteorological conditions are often ignored in favor of single-year data sets for modeling power generation and evaluating the economic value of photovoltaic (PV) power systems. Yet interannual variability significantly impacts the generation from one year to another of renewable power systems such as wind and PV. Consequently, the interannual variability of power generation corresponds to the interannual variability of capital returns on investment. The penetration of PV systems within the Hawaiian Electric Companies' portfolio has rapidly accelerated in recent years and is expected to continue to increase given the state's energy objectives laid out by the Hawaii Clean Energy Initiative. We use the National Solar Radiation Database (1998–2015) to characterize the interannual variability of the solar irradiance and meteorological conditions across the State of Hawaii. These data sets are passed to the National Renewable Energy Laboratory's System Advisory Model (SAM) to calculate an 18-year PV power generation data set to characterize the variability of PV power generation. We calculate the interannual coefficient of variability (COV) for annual average global horizontal irradiance (GHI) on the order of 2% and COV for annual capacity factor on the order of 3% across the Hawaiian archipelago. Regarding the interannual variability of seasonal trends, we calculate the COV for monthly average GHI values on the order of 5% and COV for monthly capacity factor on the order of 10%. We model residential-scale and utility-scale PV systems and calculate the economic returns of each system via the payback period and the net present value. We demonstrate that studies based on single-year data sets for economic evaluations reach conclusions that deviate from the true values realized by accounting for interannual variability.

Keywords: Interannual, Variability, Photovoltaics, Irradiance, Capacity Factor, Economics

Acknowledgments

This work was supported by the Laboratory Directed Research and Development (LDRD) Program at the National Renewable Energy Laboratory (NREL). NREL is a national laboratory of the U.S. Department of Energy Office of Energy Efficiency and Renewable Energy operated by the Alliance for Sustainable Energy, LLC. The U.S. Government retains and the publisher, by accepting the article for publication, acknowledges that the U.S. Government retains a nonexclusive, paid-up, irrevocable, worldwide license to publish or reproduce the published form of this work, or allow others to do so, for U.S. Government purposes.

Abbreviations

CF	Capacity factor
COV	Coefficient of variability
DHI	Diffuse horizontal irradiance
DNI	Direct normal irradiance
GHI	Global horizontal irradiance
PSM	Physical Solar Model
NPV	Net present value
NREL	National Renewable Energy Laboratory
NSRDB	National Solar Radiation Database
PV	Photovoltaic
SAM	System Advisory Model
TMY	Typical meteorological year

1 Introduction

Interannual variability has often been examined through the lens of the variability of the solar irradiance. Here we follow suit by considering the interannual variability of the solar resource in terms of GHI. Then, we add to the existing body of literature by extending our analysis to PV power generation at many individual sites; through a particularly fascinating case study of the State of Hawaii. The State of Hawaii is an archipelago formed by volcanic activity in the middle of the Pacific Ocean. It has diverse topologies and meteorological conditions across the archipelago and among individual islands. Located approximately 3,700 km off the coast of the continental United States, the state is entirely dependent on local electricity generation. Further, the high cost of fuel imports resulted in the highest electrical prices in the nation in 2016 (U.S. Energy Information Administration, 2016).

The State of Hawaii has been active in reforming its energy landscape. In 2015, Hawaii generated more solar electrical energy per capita from distributed facilities than any other state. During that year, solar energy from both utility-scale and distributed resources generated 35% of Hawaii's renewable electricity. As of the end of 2016, the combined Hawaiian Electric Companies, which supply power to the majority of the islands, have achieved an energy resource mix wherein 25.8% of the energy used by customers came from renewable energy resources (Viola, 2017). The penetration of solar energy is expected to continue to increase given the state's energy portfolio objectives laid out by the Hawaii Clean Energy Initiative, which commits the state to generating 100% of the electrical energy consumed across the state by renewable energy sources by the year 2045 (State of Hawaii, 2018). These are the most ambitious renewable portfolio standards laid out by any state in the nation. If executed while maintaining grid reliably, Hawaii would serve to prove the feasibility for other states that might be considering similar proposals to increase the

installed capacity of renewable energy, such as solar photovoltaic power (PV) systems.

In the U.S. market, the total capacity of PV systems has increased from 4 MW in the year 2000 to more than 40.6 GW at the end of the fourth quarter in 2016, amounting to an average annual growth rate of 68% (Perea et al., 2016). As stated in the same report, the installation rate of PV systems in the United States is projected to accelerate to more than 17 GW/year by 2022. The historic growth rate has been driven, in part, by a corresponding decrease in the installed cost of PV systems, which has reportedly fallen by more than 70% since 2010 (SEIA, 2017). In addition to the decrease in cost, policy initiatives such as tax incentives and renewable portfolio standards have contributed to these historic growth rates. Looking toward the growth in global markets, the total global installed capacity has increased from only 6.6 GW in 2006 to more than 306 GW at the end of 2016, amounting to an average annual growth rate of 47% (SolarPower Europe, 2017). The same report states that the global annual installation rate of PV systems is expected to continue to increase to between 75 GW/year and 162 GW/year by 2021. With these increased capacities, understanding the variable and resource-dependent nature of PV systems is crucial to understanding how the power network will be impacted.

The total amount of solar radiation incident on the surface of the Earth varies diurnally, seasonally, and annually. In turn, the power generated by a PV system also varies among multiple timescales. The seasonal variability of the solar resource is principally driven by the progression of the solar declination angle impacting the angle of incidence between the sun's rays and the surface of the Earth. On this timescale, short-term weather patterns are a secondary driver of variability. Regarding variability on an interannual basis, the amount of energy that the sun initially radiates into space varies through time (Kopp et al., 2005). From data presented by (Frohlich and Lean, 1998), the coefficient of variability of extraterrestrial radiation reaching the Earth's atmosphere is on the order of 0.05%. Subsequently, at each location on Earth, local climate variability further attenuates the amount of radiation that finally reaches the ground. The coefficient of variability for GHI, for instance, is much larger than the variability of extraterrestrial radiation, as will be shown in Section 3.1. Therefore, local climate variability is the primary driver of interannual variability of the local solar resource across the Hawaiian archipelago. Climate variability across the Hawaiian archipelago is caused by the combined effects the El Nino Southern Oscillation, and the Pacific Decadal Oscillation, among other major climate patterns. Understanding the variability of PV systems is critically important for grid operators because of the challenges associated with the non-dispatchable nature of PV systems, particularly the long-term interannual variability for capacity margins, reserves, and firm capacity calculations. Additionally, understanding the potential economic returns on an initial investment in PV systems is crucial for utilities and residential customers alike.

Most efforts to evaluate the economic benefits of PV systems are based on the results of a single year of energy generation data. It is often assumed that either a single year or more commonly that a typical meteorological year (TMY) data set, will be representative of all the years within the time horizon of the analysis. For example, Richard W. Wies et al. discuss the economic benefits of integrating PV systems into diesel power systems for use in remote settings. They rely on a single year of modeled PV generation and load data to calculate the simple payback time of the PV systems (Wies et al., 2004). The simple payback period is, at best, a rough gauge of the profitability by prospective PV owners, as noted by (Perez et al., 2004). The authors suggest calculating the life cycle cash flows, but they base their analysis on a single year of generation data, ignoring the reality of interannual variability. Cash flow might indeed be a better measure of the profitability of PV systems, but if the basis of the power generation model is flawed, by not accounting for interannual variability, then the conclusion built on that model might be inaccurate. The level of inaccuracy can be very large, as we show in Section 3.3. One possible reason this assumption often appears in the literature is that high-quality data spanning a long time horizon are scarce.

Generally, it is expensive to maintain high-density, ground-based solar radiation measurement arrays that record high-quality data irradiance spanning a time horizon that is long enough to make reasonable conclusions about variability on an interannual basis. For this reason, most of the existing literature examines the interannual variability of the solar resource studied via surrogate data, which is a byproduct of either climate change modeling or climate reanalysis data, rather than data from direct site measurements. For instance, Duffy et al. studied how the future climate would impact electrical generation from three renewable resources—wind, solar, and hydropower—across California. The future climate was modeled via the National Center for Atmospheric Research global climate model (Duffy et al., 2014). Fant et al. explored the interannual variability of wind and solar resources in Southern Africa. Relying on the Integrated Global Systems Model, they concluded that long-term mean solar resource potential will most likely remain unchanged by 2050; however, the solar resource expressed in terms of global horizontal irradiance (GHI) might vary by approximately 10% of the mean value on an interannual basis—i.e., yielding a regional coefficient of variability (COV) of 10% (Fant et al., 2015). Jerez et al. studied the impact of climate change on PV power generation in Europe. They relied on regional climate projections to calculate the surface down-welling shortwave radiation during 2070–2099 and data from 1970–1999 to investigate how climate change might impact PV output across Europe during a longer time horizon. Their results pointed toward a COV for GHI on the order of 2.5% in some regions (Jerez et al., 2015). Perdigão et al. approached the interannual variability of surface solar radiation over the Iberian Peninsula via ERA-40 reanalysis data to identify trends and relationships among climate variables, including solar radiation, temperature, and cloud cover (Perdigão et al., 2011).

Very few studies have approached the interannual variability of the solar resource via direct site measurements. One such study, Ereme of the Tartu Observatory in Estonia, analyzed pyranometer-based ground measurements of global and direct irradiance on seasonal timescales in Tartu-Tõravere, Estonia, to explore the interannual and intra-seasonal variability of solar radiation. Among myriad results, Ereme focused on the summer solar radiation during a 55-year span from 1955–2010 and calculated a COV for GHI on the order of 10% (Eerme, 2012). Separately, Vazquez et al. studied the interannual variability of the solar resource at Plataforma Solar de Almería, Spain, by relying on the remote sensing equipment at the DLR's radiometric station during a 9-year time series from 2001–2010 and found a regional COV for GHI on the order of 6% (Pozo-Vázquez et al., 2011).

Other approaches involved studying the interannual variability of the solar resource via the National Solar Radiation Database (NSRDB), which is produced and maintained by the National Renewable Energy Laboratory (NREL). In one case, Wilcox and Gueymard analyzed an 8-year subset of the NSRDB—specifically, the 1998–2005 version available at the time—on a 10-km by 10-km grid across the continental United States to study the interannual variability both spatially and temporally. Notably, the Wilcox and Gueymard study aimed to characterize the COV for GHI of

individual sites rather than entire regions and identified sites within the State of Washington that featured COV values ranging from a low of 0.49% to a high of 15.8% (Wilcox and Gueymard, 2010).

Generally, interannual variability has been studied under the pretext of the variability of the solar resource, expressed in terms of irradiance. In contrast to the existing literature, first we consider the interannual variability of the solar resource in terms of GHI, but then we extend our analysis to PV power generation in terms of capacity factor at many individual sites across the State of Hawaii. To underscore the significance of the interannual variability, we calculate economic returns on prospective residential-scale and utility-scale PV systems for modeled systems exposed to both low and high levels of the interannual variability of the resource. We quantify the economic returns in two ways: through the payback period, expressed with a variable model, which is in contrast to static models that use simple payback time; and through the net present value (NPV) of the PV system based on the definition described by (Short et al., 1995). Our results were obtained from analyzing the historical solar resource and meteorological conditions among the Hawaiian Islands specifically, but our final conclusions pertaining to the impact of the interannual variability should be viewed as broadly applicable to other regions across the globe.

2 Data and Methods

In this section, we describe the metrics, data sets, and analytical methods employed in this work. First, we describe the relevant factors that impact PV power generation, and we present a convenient metric for convolving these factors. Next, we discuss metrics that we use to quantify the level of interannual variability. Then, we describe the solar resource, meteorological, and, finally, power generation data sets. Last, we discuss the metrics and methods that are tapped to characterize the economic impact of the interannual variability as it relates to PV power generation.

2.1 Capacity Factor

PV power systems convert solar irradiance into usable power with a system efficiency defined as the product of the module efficiency and the inverter efficiency. The module efficiency can be well modeled as a linear function of the cell temperature, which in turn depends on ambient conditions such as air temperature, wind speed, and how well ventilated the modules are in a given arrangement (Zakaria et al., 2008). Therefore, the power generated by a PV system is a function of the instantaneous solar radiation incident on the modules, the instantaneous cell temperature, and the instantaneous inverter efficiency, with irradiance as the principal factor and all others secondary. Given that the amount of solar irradiance varies depending on the location of the system, it is useful to gauge the quality of the resource at a given location; one useful metric is the system capacity factor.

The capacity factor of a PV system is the ratio of useable power generated relative to the power that would have been generated if the system were continually operating at full capacity throughout some period. The capacity factor of a PV system communicates both the quantity of the local resource in terms of irradiance and the characteristics of the atmospheric conditions that might attenuate the solar power conversion at a given location, making this metric very useful for comparing PV systems among multiple locations and timescales.

2.2 Metrics for Characterizing Interannual Variability

Several metrics have been proposed to characterize the interannual variability of the capacity factor of PV systems, including the COV, which is a standardized measure of the dispersion of a sample of data about the sample mean, often expressed as a percentage, and is defined as follows:

$$\text{COV} = \frac{\sqrt{\frac{1}{n} \sum_{i=1}^n (a_i - \bar{a})^2}}{\bar{a}} \cdot 100\% = \frac{s}{\bar{a}} \cdot 100\% \quad (1)$$

Here, s is the sample standard deviation, and \bar{a} is the mean of n sample points (Habte et al., 2014). Throughout the remainder of this paper, COV means the COV of the sampled variable on an interannual basis, meaning that n , in Equation 1, represents the number of years sampled, and a_i represents the value of the random variable of interest during a sample year. This is said simply in theory; in practice, the process of collecting enough sample data to characterize the COV can be challenging. The dispersion of sampled data can also be characterized via interquartile ranges, taken at every 25th percentile, or by calculating the range of the data. Our summary tables throughout Section 3 report each of these metrics.

2.3 Solar Resource and Meteorological Data

High penetration levels of solar renewable energy and economically optimal system designs are enabled through the availability of accurate knowledge of the quantity and variability of the solar resource at a given location. The U.S Department of Energy has funded the multiyear cultivation of the NSRDB. The NSRDB has been updated three times since being released in 1992, culminating in the most recent version, NSRDB (1998–2015) (Habte et al., 2017).

In contrast to ground-based sensing equipment, such as widely scattered pyranometer and pyrhemliometer arrays, satellite-based observations can yield high-density measurements of atmospheric conditions and reflected radiation, which can, in turn, be used to generate high temporal and spatial resolution gridded estimates of surface radiation for long periods of time. To further the advantages that satellite-based measurements hold compared to ground-based measurements, NREL developed the physics-based Physical Solar Model (PSM). The PSM was supplied with satellite data to generate gridded GHI, direct normal irradiance (DNI), and diffuse horizontal irradiance (DHI) for the NSRDB at a 4-km by 4-km spatial resolution and half-hourly temporal resolution covering the 18 years from 1998–2015. The current version includes an area bounded by the 25°W and 175°W meridians and by the -20°S and 60°N parallels. In addition to irradiance data, the NSRDB contains other relevant meteorological data sets, including wind speed and temperature taken from NASA's MERRA data set (Rienecker et al., 2011) after interpolating from a 40-km by 40-km grid down to match the 4-km by 4-km spatial resolution of the NSRDB. The NSRDB also contains typical meteorological year (TMY) data sets that were generated via a modified version of the Sandia National Laboratories method for compiling an annual time series with variability consistent with

long-term observations (Janjai and Deeyai, 2009). TMY data sets are composites of monthly time series from multiple years to form a single-year time series, and they are often relied upon for energy system modeling to relax the need for multiyear problem formulations. Although they are convenient for reducing the dimensionality of modeling problems, TMY data sets fail to reflect the consequences of interannual variability as it relates to energy generated from PV systems. The limitations of TMY data sets for representing solar irradiance data are discussed in great detail in (Vignola et al., 2012) wherein the authors point out that there is no guarantee that the TMY3 data sets will be an accurate representation of the average irradiance over a larger period of record.

The performance of the PSM-based irradiance data sets in the NSRDB (1998–2015) was evaluated in (Habte et al., 2017). The report demonstrates that the hourly average satellite-derived data have a mean bias error of $\pm 5\%$ for GHI and less than $\pm 10\%$ for DNI when compared against concurrent ground-based measurements from seven sites of the Surface Radiation Budget Network. Further, the same report demonstrates the ability of the NSRDB to accurately feature interannual variability by comparing the COV for both the PSM data sets and ground-measured from seven Surface Radiation Budget Network stations across the United States; on average the data sets differ by only 0.68% COV for GHI and 0.97% COV for DNI and show similar annual trends. The root mean squared residuals between the MERRA data sets and measured data were reported in (Rienecker et al., 2011). The MERRA data sets were also independently evaluated in (Pfeifroth and Mueller, 2012), (Yi et al., 2011), and (Jones et al., 2016); the data sets have a mean temperature bias of less than 1°C globally. In this study, we use the NSRDB (1998–2015) to sample 1-hour resolution DHI, DNI, temperature, and wind speed data among the Hawaiian Islands for the 18 years available. Additionally, we use the TMY data sets that are available in the NSRDB, specifically the third and most recent version of the TMY data contained in the NSRDB, TMY3.

The amount of the solar irradiance at a given location and the temperature at that location are the primary and secondary factors that impact the instantaneous power output of PV systems. GHI values are often reported in a way that excludes values below a certain threshold of the clear-sky radiation. This excludes the shading effect that is pronounced during the early morning and late evening hours. We calculated the first nonzero GHI value during each day, for each site across the State of Hawaii; the mean value was 65.4W/m^2 . Therefore, when characterizing the variability of GHI, values less than 65W/m^2 have been excluded to ignore the shading effects. This compares well with a value obtained from a regression analysis contained in another work; a value of 60W/m^2 was used to exclude the shading effects (Lave and Kleissl, 2010). In addition to these temporal exclusions, spatial exclusions are also considered and explained in the next section.

2.4 Spatial Exclusions

Several spatial constraints are introduced when extending the analysis from solar resource to PV power generation. Spatial constraints to solar power development may be present across different parts of the globe. For example, a utility, or a homeowner, would not be able to build a PV plant or PV array on protected lands, on city streets, in flood zones, or on farmland and would also be subject to local spatial constraints, lava flows in Hawaii for instance. Spatial exclusion analyses have been considered in several studies in the literature that explore the potential for utility-scale wind farms, solar plants, and other energy systems. Some examples include (Elliott et al., 1991), (Karsteadt et al., 2005), (Hoogwijk et al., 2005), and (Haaren and Fthenakis, 2011).

The vertices of the 4-km by 4-km NSRDB grid coincide with the centroids of 16-km^2 cells. In this study, it is assumed that the solar radiation and meteorological conditions within a cell are homogenous and equal to that at the centroid. First, the interannual variability of the GHI, meteorological conditions, and capacity factor of PV systems is characterized to explore the how these values vary across each island. Within a cell, there might be locations that fall within the boundaries of protected lands or happen to have topologies that are not suitable for building PV power systems. To address this reality, we established criteria to determine whether a location is suitable for building utility-scale PV systems and to exclude locations that are not (see Figure 1). Regarding the terrain slope, the maximum slope that would be suitable for building utility-scale PV before potentially incurring additional capital costs is 5% (HECO, 2016). According to the same report, terrain slopes of up to 10% might be developable, although this would require additional capital investment to prepare the site. Since evaluating the maximum PV resource potential across the Hawaiian Islands is not our objective in this work, we restrict our analysis to terrain slopes less than or equal to 5% to eschew complications to subsequent economic analysis. The proportion of land within an NSRDB cell that fails to meet these criteria is calculated so that the power generation data set can be scaled to account for the various spatial exclusions. Then the exclusions are applied to restrict the discussion of capacity factor of utility-scale PV systems which could be feasibly built.

The criteria are as follows:

- Contiguous areas of 1 km^2
- Terrain slope $\leq 5\%$ ¹
- Not part of U.S. National Park Service or Hawaii State Park land²
- Not U.S. Fish and Wildlife Service land³
- Zoning exclusions:⁴
 - Not zoned as an urban area
 - Not classified as important agricultural land

¹ We relied on the National Elevation Datasets to define the slope exclusion zones that were obtained through the U.S. Geological Survey (nationalmap.gov).

² The zones defined as U.S. National Park Service and Hawaii State Parks can be obtained from the U.S. National Park Service website (nps.gov/state/hi).

³ The U.S. Fish and Wildlife Service zones have been consolidated into a single data set that is made available through the Hawaii Office of Planning Global Information Systems website (geportal.hawaii.gov).

⁴ The land zoning, flood zones, and lava flow hazards are also available through the Hawaii Office of Planning Global Information Systems website (geportal.hawaii.gov).

- Not designated as an agricultural Zone A
- Not within an A(x)-level flood zone
- Not within a lava flow hazard Zone 1 or Zone 2
- Not classified as wetland.

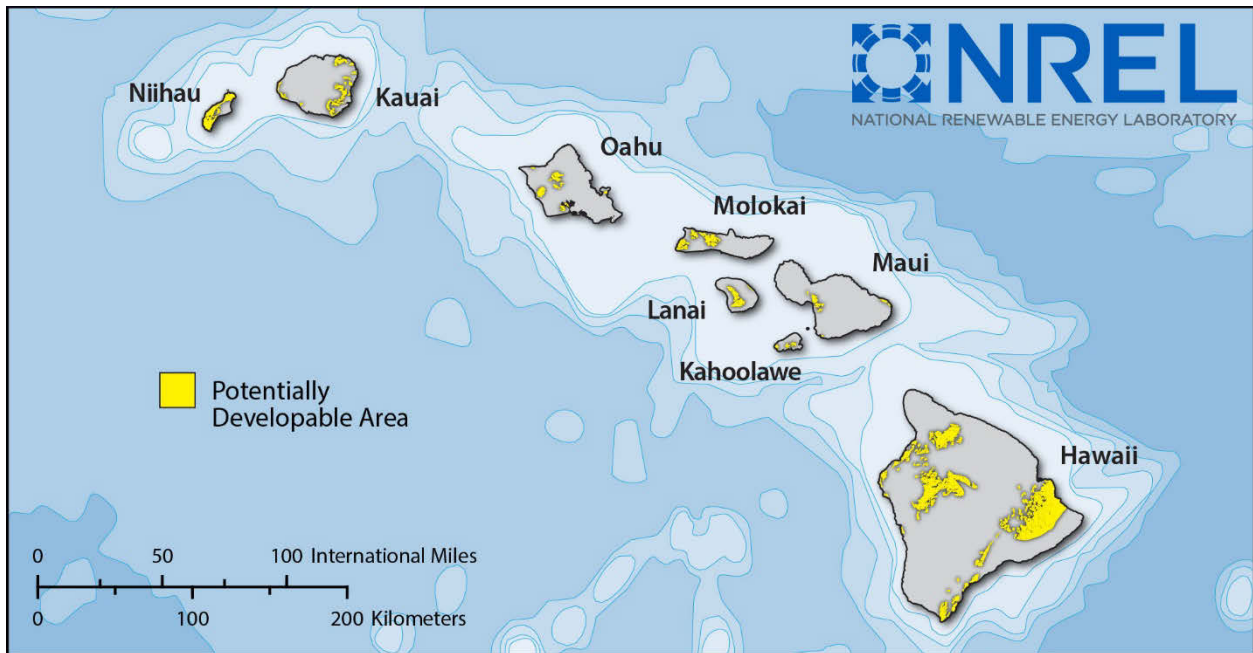


Figure 1: Zones that meet the criteria for suitability for constructing utility-scale photovoltaic power plants.

2.5 Power Generation Data Set

The solar irradiance and meteorological NSRDB data sets from 1998–2015 were used to calculate a corresponding 18-year power generation data set using NREL’s System Advisory Model (SAM). SAM is a computer model that can calculate the technical performance as well as the economic impact of renewable energy systems (Blair et al., 2014). The technical performance is evaluated as the total energy generated by a system defined with certain technical parameters when subject to meteorological and resource conditions. The set of technical parameters that are necessary as inputs to the model depends on the version of SAM being used. In this study, we use SAM PVWatts Version5 (Dobos, 2014). SAM PVWatts was validated in (Freeman et al., 2013) against measured data from nine PV system configurations, including eight fixed tilt systems and one single axis tracking system. The validation was repeated for SAM PVWatts 5 in (Dobos, 2014); PVWatts 5 reportedly under-predicts system performance by only 1.8% as compared to 11.9% for Version1. PVWatts 5 assumes certain technical parameters based on the nameplate capacity of a modeled system. For example, the inverter size that is necessary for a given PV array is calculated based on the size of the array rather than a manual model input parameter. Similarly, the type of PV cell is not explicitly specified by the user; instead, for the efficiency calculations, SAM uses physics-based models to calculate the efficiency parameters that are characteristic of a typical PV module commercially available today. The model considers solar irradiance in the form of DNI and DHI as well as wind speed and ambient temperature to calculate the PV module efficiency as well as the energy generated during a given instance. SAM PVWatts 5 allows for a convenient way to generate realistic power data from solar resource and meteorological data. The benchmark PV system configuration used to obtain 18 annual capacity factor values for each NSRDB cell is a 1-axis tracking PV system with tilt fixed at 0 degrees and an inverter DC-AC ratio of 1.2, all of which was selected to represent a utility-scale system. We define a residential system to be a 5-kW DC array on a 30-degree, fixed tilt mounted to a roof, chosen to represent the typical roof pitch, and oriented on a 180-degree azimuth. We define a utility-scale system as a 5-MW DC, 0-degree tilt, on a 1-axis tracking array, oriented on a 180-degree azimuth. In Section 3.3, in which the analysis spans several sequential years, all systems are modeled with annual system degradation of 0.5%.

Sensitivities were performed that revealed that the interannual variability does not depend on the DC-AC ratio, even though the capacity factor is impacted. We compare two tracking configurations: we calculate the capacity factor for the utility-scale PV system assuming that the system is a single-axis tracking system and, separately, a 20-degree, fixed-tilt system. The single-axis tracking systems generally yield a larger annual capacity factor; however, this has little impact on the COV for annual capacity factor. We also explore the sensitivity of the annual capacity factor to the DC-AC ratio assumed for the inverter. This seems to have very little impact on the average annual capacity factor. More details on these sensitivities can be found in Appendix A.

2.6 Characterizing Economic Impact of Interannual Variability

We aim to underscore how interannual variability impacts economic decision-making as it relates to the value of potential PV systems when considering both residential-scale systems and utility-scale systems. We calculate the payback, defined in years, and the NPV of arrays built at locations on the two sides of the Island of Hawaii, east and west, to account for the effects of geographical variability. We use the definitions for payback and NPV presented in (Short et al., 1995). The calculation of NPV depends on several economic parameters, including the economic discount rate, inflation rate, debt ratio, and interest rate. For each of the relevant parameters, we select values to match SAM’s residential and

commercial financial models.⁵ The east and west side of the Island of Hawaii receive very different amounts of annual rainfall; the eastern side receives a mean rainfall of 260-300 inches whereas the western side receives only 8-30 inches (Frazier et al., 2016). Therefore, on each side of the island, two locations with similar 18-year mean capacity factors but with very different COV values are identified. In this way, we compare the economic payback and NPV of potential PV systems at locations with varying levels of interannual variability while accounting for differences in weather conditions.

We perform four economic analyses for each of the four locations. First, we calculate the payback period in years and the NPV that would correspond to a system that generated power throughout the years 1998–2015. Therefore, in the first analysis, we model the true historical power output of the PV system in a multiyear consideration to serve as a baseline. For the remaining analyses, we calculate the payback period and NPV associated with projecting a single-year data set through the 18-year time frame—i.e., assuming that each year features identical solar resource and meteorological attribute time series—to highlight some of the deficiencies associated with single-year forward projections. We consider three cases of single-year forward projections: a projection of the year featuring the least resource and consequently the lowest capacity factor; the year with the most resource and consequently the highest capacity factor; and, finally, the TMY data set.

3 Results and Discussion

Our results are presented as follows: in Section 3.1, we consider the variability of the solar resource in terms of GHI and of the meteorological variables across the state, without spatial exclusions applied. In Section 3.2, we discuss the interannual variability of PV power generation after using SAM to calculate our power generation data set; the analysis is repeated before and after weighing the mean values from all the included NSRDB cells by land availability. In Section 3.3, we underscore the impact of the interannual variability on economic decision-making.

3.1 Interannual Variability of Local Solar Resource and Temperature

The monthly average of hourly solar resource data for all sites across the State of Hawaii is calculated for the years 1998–2015. Each of the islands in the Hawaiian archipelago was considered independently. Figure 2 and Figure 3 present the results for the Island of Hawaii alone; however, annually aggregated results for the remaining islands are tabulated separately in (Bryce et al., 2018).

As shown in Figure 2 and Figure 3, there is significant interannual variability of the solar resource across the Island of Hawaii. The solar resource varies to the extent that the range of levels during the summer overlaps with those during the winter; the mean GHI level for January 2001 was larger than that for August 2000, 2002, and 2015. The years featuring the largest consecutive change annual mean GHI level occurred between 2009 and 2010, with an increase of 5.6% from one year to another. The year 2003 featured the highest average daytime level, with GHI at 466.7W/m². The year 2009 featured the lowest average daytime level, with GHI at 441.3W/m².

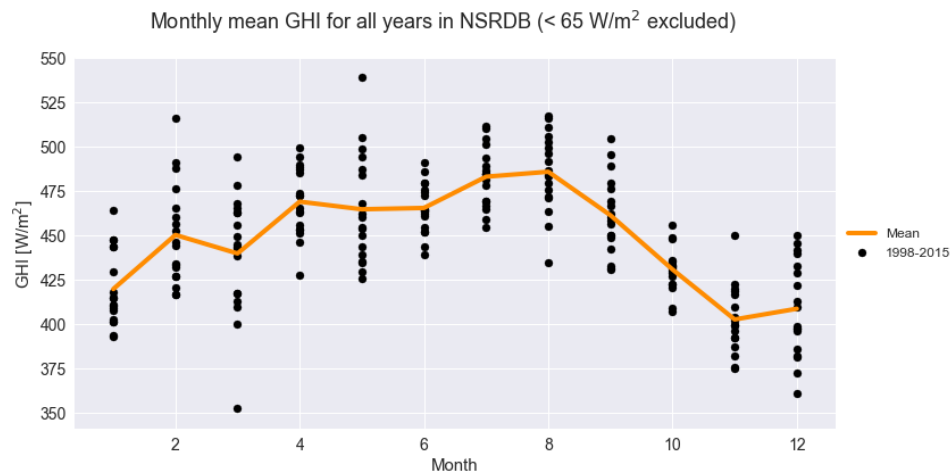


Figure 2: Monthly mean daytime global horizontal irradiance (W/m²) across the Island of Hawaii for 1998–2015.

⁵ More information on the financial models is readily available at sam.nrel.gov/financial.

Monthly mean GHI for all years in NSRDB (< 65 W/m² excluded)

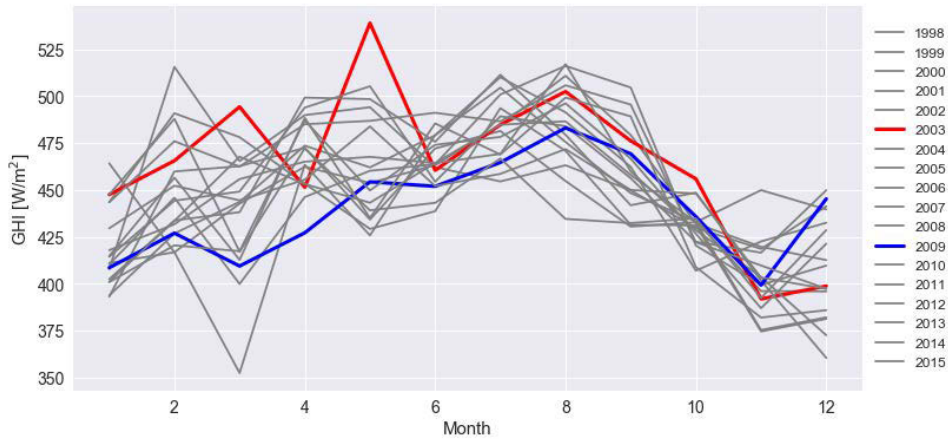


Figure 3: Monthly mean daytime global horizontal irradiance (W/m²) across the Island of Hawaii for 1998–2015. Years with the minimum (maximum) annual average resource are highlighted in blue (red).

The mean, COV, and range of the monthly average GHI values are highlighted in Table 1. The bottom row communicates the annual mean values obtained by averaging the daily values throughout the year. The summary statistics are calculated on an interannual basis. For example, the COV value listed for the annual mean values is, therefore, the COV of the annual means, which communicates a different metric than the COV values for the monthly mean values. For this reason, the COV values for the monthly means fall within the range of 2.89%–7.65%, and separately the COV value for the annual mean GHI is 1.73%. Within the historical data analyzed here, the annual mean value of the GHI varies less than the monthly mean values on the same basis. The greatest degree of interannual variability was observed for the month of March, and the smallest degree of variability was observed for the month of June, suggesting that the GHI values observed during the late winter vary more on an interannual basis than those during the midsummer values across the Island of Hawaii. Similar tables have been generated for all eight islands of the archipelago, and those results are listed in (Bryce et al., 2018).

Table 1: Monthly mean global horizontal irradiance (W/m²) across the Island of Hawaii for 1998–2015 with statistical summaries. Color scheme for monthly values separated for every 25th percentile. Years with the minimum (maximum) annual average resource are outlined in blue (red).

Month	1998	1999	2000	2001	2002	2003	2004	2005	2006	2007	2008	2009	2010	2011	2012	2013	2014	2015	Q1	Mean	Q3	Sdev	COV	Min	Max	Range
January	443.5	393.7	407.7	464.2	393.0	447.5	410.4	414.4	411.0	402.4	417.8	408.5	443.4	401.0	429.5	414.8	400.8	447.5	403.7	419.5	440.0	21.2	5.05%	393.0	464.2	71.1
February	490.9	426.8	515.6	416.7	459.8	465.6	445.8	444.2	416.8	433.7	431.7	426.9	476.0	433.5	452.2	456.5	420.4	487.9	428.1	450.1	464.1	28.2	6.27%	416.7	515.6	98.9
March	478.1	443.6	465.4	442.7	462.7	494.3	399.9	449.2	352.4	438.1	455.8	409.4	462.4	467.7	444.4	412.7	417.3	417.0	417.1	439.6	462.6	33.6	7.65%	352.4	494.3	141.9
April	453.3	473.6	489.9	462.4	472.5	451.4	446.2	493.9	463.4	499.2	465.1	427.1	485.0	453.1	455.4	488.4	487.0	472.2	453.8	468.8	486.5	19.3	4.12%	427.1	499.2	72.1
May	429.2	462.0	494.1	453.7	434.2	539.0	460.2	505.3	425.7	498.4	467.6	454.3	486.8	443.2	483.8	435.0	449.7	439.1	440.1	464.5	486.1	30.9	6.65%	425.7	539.0	113.2
June	438.6	479.1	462.2	463.3	472.1	460.4	463.7	454.4	479.2	475.7	464.3	451.9	491.1	464.4	452.1	485.5	474.0	443.1	455.9	465.3	475.3	14.2	3.04%	438.6	491.1	52.5
July	493.6	504.5	454.5	484.4	481.4	484.8	500.9	489.3	510.1	511.4	469.2	464.6	486.5	484.8	458.6	468.9	478.3	466.7	469.0	482.9	492.5	17.0	3.52%	454.5	511.4	56.9
August	470.8	475.6	463.1	510.9	454.7	502.5	516.1	484.0	491.4	479.4	517.1	483.1	505.8	486.6	471.8	499.3	496.2	434.5	472.7	485.7	501.7	22.0	4.52%	434.5	517.1	82.5
September	431.4	448.3	449.8	479.3	430.4	476.2	504.6	456.3	462.3	441.8	459.9	469.3	495.5	458.0	450.0	489.2	466.6	432.3	448.7	461.2	474.4	21.7	4.70%	430.4	504.6	74.2
October	431.1	433.3	429.7	432.1	432.8	455.9	420.3	422.3	406.9	448.5	428.5	435.8	422.1	432.8	448.1	408.9	426.6	434.8	423.4	430.6	434.4	12.4	2.89%	406.9	455.9	49.0
November	374.5	396.0	418.5	419.7	449.9	391.9	399.4	416.5	422.5	401.6	403.5	399.2	409.7	375.3	403.3	381.9	386.9	392.4	392.0	402.4	414.8	18.7	4.64%	374.5	449.9	75.4
December	381.2	395.9	441.2	412.6	439.6	398.7	409.6	449.8	432.5	360.4	372.5	445.2	397.3	382.0	397.3	385.9	421.3	428.5	388.4	408.4	431.5	26.9	6.59%	360.4	449.8	89.4
Annual Mean	444.9	447.8	458.8	455.7	449.7	466.7	450.9	458.7	442.4	453.2	449.2	441.3	465.9	443.0	447.6	446.7	446.6	441.9	445.3	450.6	455.1	7.8	1.73%	441.3	466.7	25.4

As mentioned in Section 2.1, the ambient temperature affects the conversion efficiency of a PV module. The conversion efficiency decreases by an amount on the order of 0.5% for every degree shift from the standardized reference cell temperature of 25°C (Dubey et al., 2013). This would not be an instantaneous process, but it could certainly occur during the span of hours, which is within the time resolution of the NSRDB data sets used here. The cell temperature varies with several factors, including the irradiance incident on the cell surface and by the ambient temperature. For this reason, we characterize the interannual variability of the ambient temperature at each site. Each of the islands of the Hawaiian archipelago was considered independently from one another, and annually aggregated results are tabulated in (Bryce et al., 2018). As was the case for the solar resource, we note significant interannual variability in the temperature data. For the Island of Hawaii, we calculated a COV value for temperature of 2.02%.

3.2 Interannual Variability of Photovoltaic Power Generation

Here we discuss the interannual variability of PV power generation. The 18-year mean of capacity factor and values for all sites among the Hawaiian Islands were calculated (see Figure 4). Interestingly, both the minimum and maximum values are observed on the largest island in the archipelago, the Island of Hawaii, with values of 10.8% and 27.1%, respectively. Note that this island hosts a volcano with a peak elevation of 13,796 ft (4,205 m) above sea level. The peak is almost always above the cloud line, resulting in the high capacity factor values observed. For that matter, the volcano is the source of the clouds: as the moist air from the oceanic trade winds is pushed upward by the volcano, the water condenses, forming clouds that then blanket the east side of the island. These clouds eventually release their water as rain on the east side of the island, or colloquially, “the rainy side.” The cloud cover results in less solar irradiance on this side of the island, as shown in Figure 4, and increased variability overall.

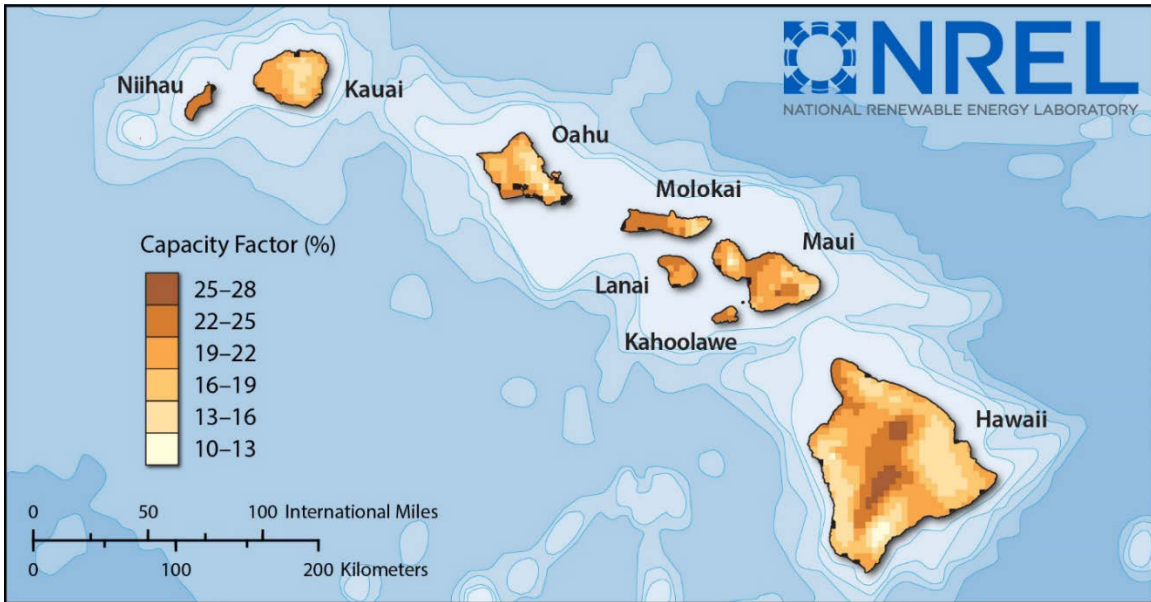


Figure 4: The 18-year mean of capacity factor values of utility-scale, 1-axis tracking PV systems with tilt fixed at 0 degrees and an inverter DC-AC ratio of 1.2 among the Hawaiian Islands.

To investigate the interannual variability of the capacity factor values, we calculate COV from the 18 annual capacity factor values (see Figure 5). As expected, the largest island hosts sites with the highest level of variability with a COV value of 14.1%. The smaller islands generally exhibit less interannual variability. Sites with high levels of interannual variability are observed on the eastern side of most of the larger islands. Note that for the bulk of sites, the COV value of the capacity factors are within a range from 0%–7.5% and very few sites are outside of this range. Considering that the median value for COV is 3.5%, this translates to a 5-kW rated residential PV array at a location with an average capacity factor of 20% generating between marginally more than 7,800 kWh and slightly less than 6,800 kWh of usable electricity on from one year to another.

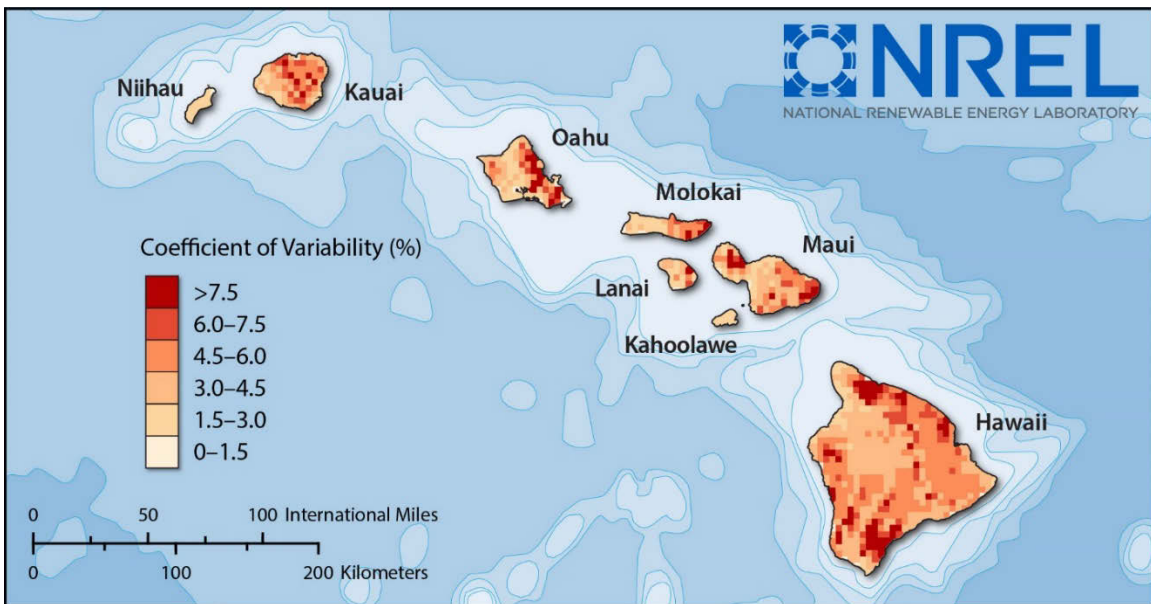


Figure 5: Coefficient of variability of annual capacity factor of photovoltaic system values from 1998–2015 among the Hawaiian Islands.

It is useful to inspect the site-specific distribution of the capacity factor for each year. These distributions are unique to the island being considered (see Figure 6). Not only do the interquartile ranges vary on an interannual basis but the extreme points of the distributions also vary on an interannual basis. Islands with a larger area, such as Hawaii and Maui, yield broader ranges of capacity factors on a site-specific basis than smaller islands such as Niihau; we calculate the standard deviation of the distributions of capacity factor across the Island of Hawaii to be 3.5% and 0.6% for Niihau. The mean values of the distributions also vary by island. The smaller islands lack large changes in elevation which would promote cloud formation, explaining the reduced overall variability and increasing the mean capacity factor. Additionally, smaller islands feature less persistent cloud cover since passing weather events move over the smaller islands quicker than larger islands. It follows that the size scale, and therefore small sample sizes of the smaller islands, may play a role in reducing the overall variability during any given year. In contrast, the relatively lower mean

capacity factor and higher overall variability among the larger islands can be explained by considering their diverse topologies, including large volcanoes that cast shadows during dawn and dusk and support microclimates with more persistent cloud cover than the smaller islands.

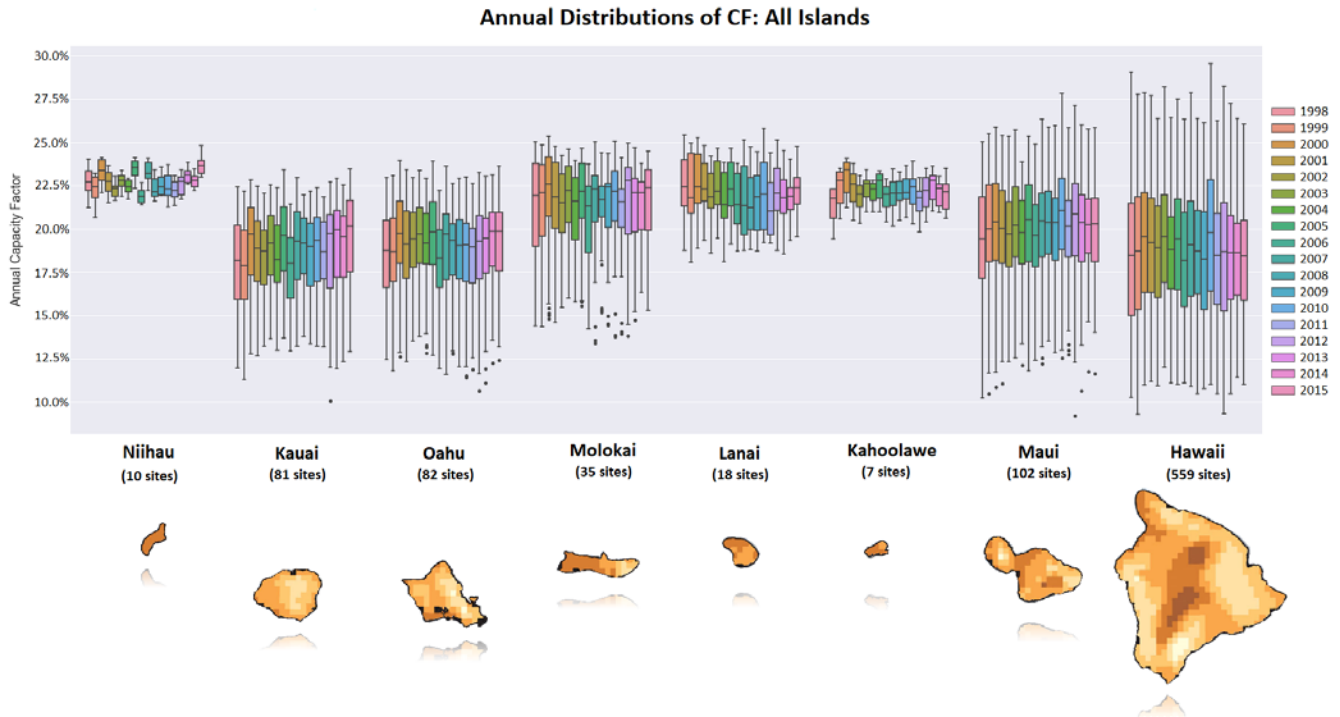


Figure 6: Distribution of annual mean capacity factor among all sites for the years 1998–2015, repeated for each island. Outliers beyond 150% of the interquartile range are shown as dots.

To focus the discussion of capacity factor to utility-scale PV systems which could be feasibly built, we apply the spatial exclusions based on the exclusion criteria, as discussed in Section 2.4, and we inspect the capacity factor values among the included zones across the Island of Hawaii and the interannual variability in terms of COV of the annual capacity factor calculated for the years 1998–2015 (see Figure 7). Following this procedure, the range of capacity factors and COV values generally decreased across each island. For example, across the Island of Hawaii, the range of capacity factors narrowed by 3.6% and the range of COV values narrowed by 1.2% after the spatial exclusions were applied.

We notice that the capacity factor and COV are inversely correlated, suggesting that sites with a lower 18-year mean of capacity factor tend to exhibit more interannual variability in terms of COV, both with and without spatial exclusions across the Hawaiian Islands. This effect cannot be explained by random variability alone. Rather, the inverse correlation between the capacity factor of a given site and the COV at that site is significant based on the Pearson’s correlation coefficient, as shown in Figure 8. Sites featuring a capacity factor level 10% less than another site generally feature 3% more interannual variability, expressed in terms of COV. A low capacity factor value indicates that solar irradiance is attenuated by cloud cover, which drives more variability at a given location on both a monthly and interannual basis.

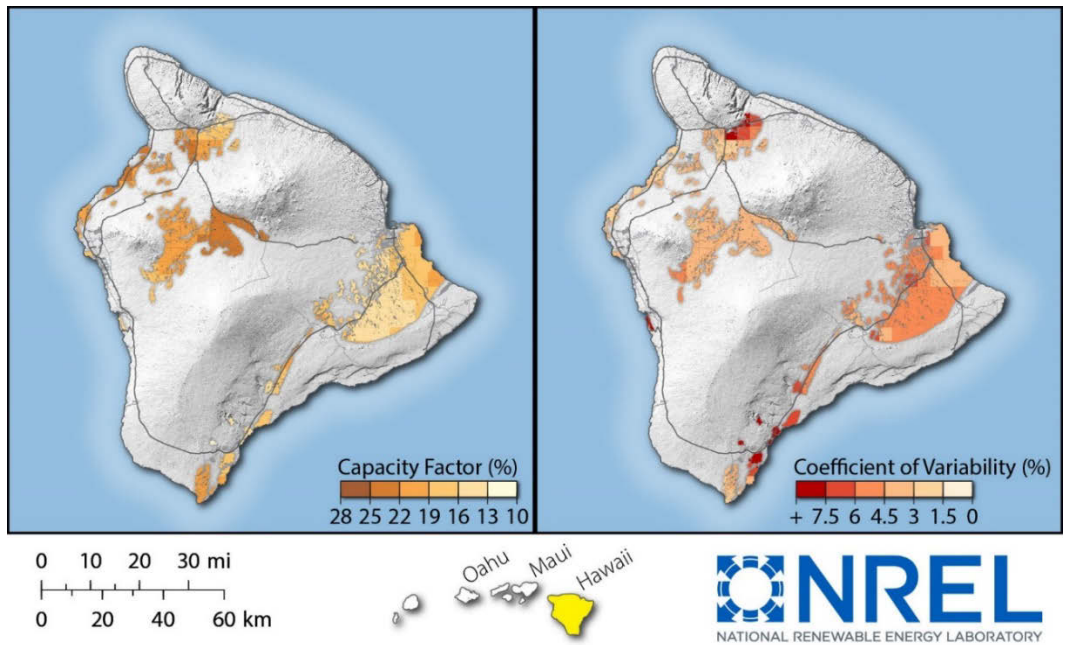


Figure 7: (Left) The 18-year mean of capacity factor values of 1-axis tracking photovoltaic systems with tilt fixed at 0 degrees and an inverter DC-AC ratio of 1.2 for all zones suitable for constructing utility-scale photovoltaic systems across the Island of Hawaii. (Right) The coefficient of variability of annual capacity factor values from 1998–2015.

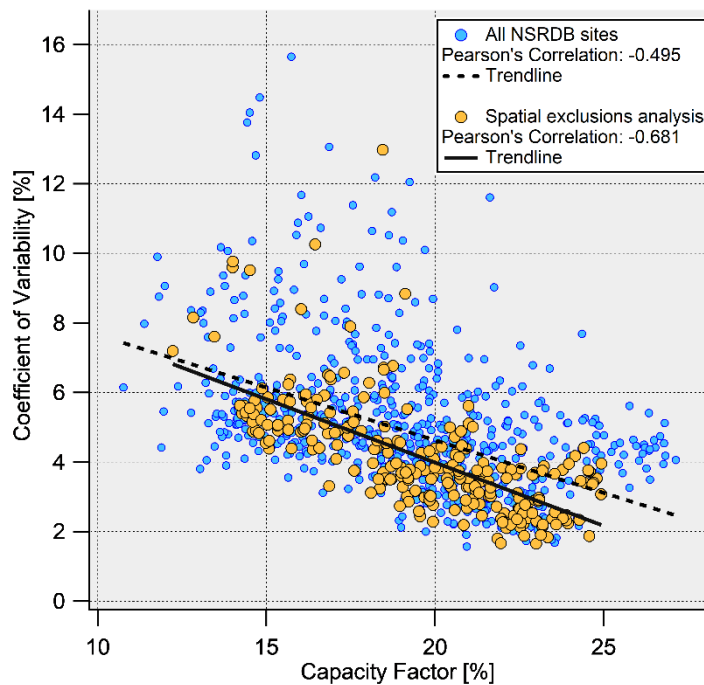


Figure 8: Scatter of coefficient of variability against capacity factor for all NSRBD sites, and following the spatial exclusion analysis, across the Hawaiian Islands. Pearson's correlation statistics are shown. The trend line of the coefficient of variability versus the capacity factor is shown.

Table 2: Monthly mean capacity factors across the Island of Hawaii from 1998–2015 with statistical summaries. Color scheme for monthly values separated for every 25th percentile. Years with the minimum (maximum) annual average resource are outlined in blue (red).

Month	1998	1999	2000	2001	2002	2003	2004	2005	2006	2007	2008	2009	2010	2011	2012	2013	2014	2015	Q1	Mean	Q3	Sdev	COV	Min	Max	Range
January	18.2%	14.9%	15.7%	19.2%	15.0%	18.1%	16.1%	16.2%	15.6%	15.3%	16.8%	16.2%	17.7%	15.4%	17.2%	16.6%	16.2%	17.7%	15.6%	16.6%	17.6%	1.2%	7.40%	14.9%	19.2%	4.3%
February	19.5%	16.3%	21.2%	15.9%	18.1%	18.3%	17.5%	17.5%	16.3%	16.7%	16.7%	16.3%	18.9%	17.4%	17.7%	18.0%	16.7%	19.8%	16.7%	17.7%	18.3%	1.4%	8.02%	15.9%	21.2%	5.3%
March	20.4%	18.0%	19.8%	18.8%	19.7%	21.2%	16.0%	18.3%	12.9%	18.6%	19.3%	15.9%	19.1%	18.8%	17.4%	16.6%	17.3%	16.4%	16.8%	18.0%	19.2%	2.0%	10.95%	12.9%	21.2%	8.3%
April	18.6%	19.9%	20.1%	19.4%	19.5%	18.4%	19.3%	20.8%	19.1%	21.5%	19.5%	16.6%	20.4%	18.7%	18.7%	20.5%	20.2%	20.0%	18.8%	19.5%	20.2%	1.1%	5.65%	16.6%	21.5%	4.9%
May	17.9%	19.8%	22.0%	20.8%	19.2%	23.7%	20.6%	23.2%	18.4%	22.1%	21.3%	19.9%	21.4%	19.0%	21.1%	19.5%	20.9%	19.1%	19.3%	20.6%	21.4%	1.6%	7.80%	17.9%	23.7%	5.8%
June	19.7%	22.5%	22.0%	20.8%	22.0%	22.0%	21.5%	21.0%	21.9%	22.2%	21.2%	21.0%	22.5%	20.8%	20.4%	21.8%	22.6%	21.0%	21.0%	21.5%	22.0%	0.8%	3.73%	19.7%	22.6%	2.9%
July	22.1%	23.3%	20.2%	22.4%	21.2%	21.8%	23.9%	21.9%	22.5%	23.4%	22.2%	20.6%	22.8%	22.4%	20.7%	21.2%	20.5%	21.9%	21.2%	22.0%	22.5%	1.0%	4.77%	20.2%	23.9%	3.7%
August	20.3%	20.6%	19.5%	22.3%	19.3%	22.1%	23.3%	21.6%	21.3%	21.4%	22.8%	21.0%	22.4%	20.9%	20.2%	22.5%	22.2%	18.9%	20.3%	21.3%	22.3%	1.3%	5.97%	18.9%	23.3%	4.4%
September	18.2%	19.9%	19.6%	20.3%	18.3%	20.9%	22.7%	19.0%	19.5%	18.7%	20.5%	19.5%	21.4%	19.5%	18.8%	21.7%	20.8%	18.2%	18.8%	19.9%	20.8%	1.3%	6.52%	18.2%	22.7%	4.5%
October	17.7%	18.0%	17.2%	17.6%	17.7%	19.1%	17.2%	17.5%	16.9%	18.7%	17.2%	18.1%	17.5%	17.8%	18.7%	16.6%	17.2%	18.3%	17.2%	17.7%	18.1%	0.7%	3.76%	16.6%	19.1%	2.5%
November	13.7%	14.8%	15.3%	15.4%	18.4%	15.0%	15.5%	16.5%	16.8%	15.4%	15.3%	15.0%	16.4%	13.9%	15.0%	14.0%	14.4%	15.0%	14.8%	15.3%	15.4%	1.1%	7.42%	13.7%	18.4%	4.7%
December	13.7%	14.3%	17.0%	15.4%	16.8%	14.8%	14.8%	17.4%	15.8%	12.6%	13.2%	16.7%	14.7%	14.0%	14.4%	14.3%	15.4%	16.1%	14.3%	15.1%	16.1%	1.4%	8.99%	12.6%	17.4%	4.8%
Annual Mean	18.3%	18.5%	19.1%	19.1%	18.8%	19.6%	19.1%	19.3%	18.1%	18.9%	18.9%	18.1%	19.6%	18.2%	18.4%	18.6%	18.7%	18.5%	18.4%	18.8%	19.1%	0.5%	2.49%	18.1%	19.6%	1.6%

Comparing Table 1 and Table 2 shows that the highest and lowest levels of capacity factor, after the spatial exclusions were applied, were observed during the same year as the highest and lowest levels of GHI, respectively, as expected. The capacity factors follow a regular seasonal trend each year, but with significant interannual variability during any given month. Figure 9 shows that the mean capacity factor among all sites of the Island of Hawaii varies to the extent that the range of levels during the summer overlap with those during the winter. Similar tables have been generated for all eight islands of the archipelago, and those results are listed in Appendix A.

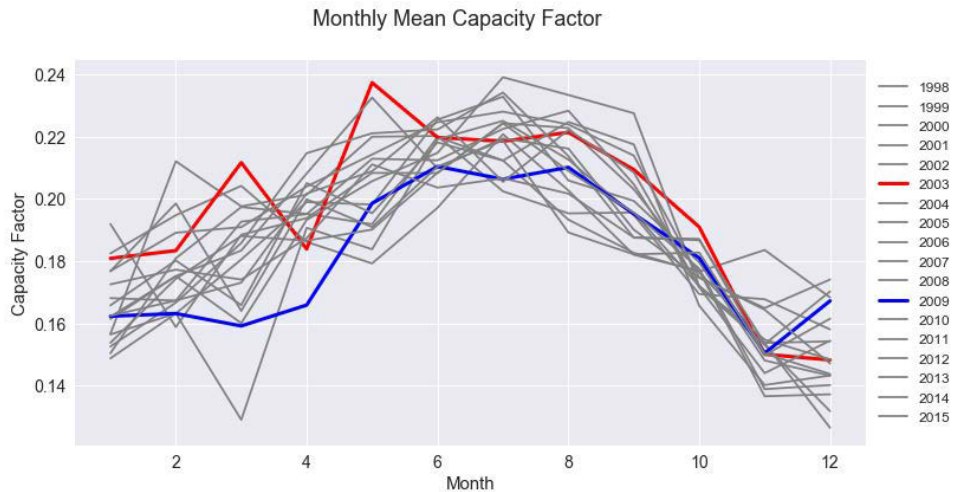


Figure 9: Monthly mean capacity factor for 1998–2015. Spatial exclusions have been applied. Years with the minimum (maximum) annual average resource are highlighted in blue (red).

The number of years that are included in the analysis impacts the calculated COV value corresponding to a given location. To demonstrate this, we sample all possible subsets of CF values from various numbers of years and calculate the COV value for each subset. For example, from the eighteen annual mean CF values in Table 2, there are 153 unique combinations that can be constructed from two-year subsets to be used to calculate a COV value. Then, for a given number of years constituting the subsets, we calculate the average and variance of the COV values and plot the results in Figure 10. The COV values converge as larger subsets -more years- are considered, meaning that the COV can be fairly characterized by sampling some number of years, with that number being dependent on the objective of the analysis being performed. As an example, the variance of the COV values falls below 0.5% when sampling 7 years of the available data, whereas the variance of the COV values falls below 0.25% when 13 years are sampled. Regardless of the level of uncertainty that is acceptable for a given analysis, the COV values converge as more years are considered.

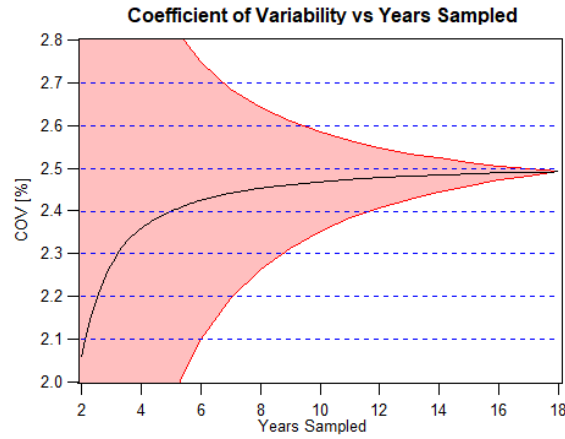


Figure 10: Convergence of the coefficient of variability calculated via the combinatorial subsets of the annual island-wide average capacity factors. Spatial exclusions have been applied. The variance of the COV values is shown as the shaded band.

Because of large populations, it is interesting to inspect the 18-year mean system capacity factors for the islands of Maui and Oahu along with the COV of the system capacity factors among the zones that meet the criteria for building utility-scale PV systems, as shown in Appendix A in Figure A-5 and Figure A-6. The system capacity factor values vary to a lesser degree for these islands than those across the Island of Hawaii. Averaging across the Island of Maui, we observe an 18-year mean system capacity factor of 22.5% with a corresponding COV of 2.20%. Across the island of Oahu, we observe an 18-year mean system capacity factor of 20.2%, which is slightly less than that of Maui, with a corresponding COV of 1.93%.

3.3 Economic Impact of Interannual Variability

We aim to underscore how interannual variability impacts economic decision-making as it relates to the value of potential PV systems considering both residential-scale systems and utility-scale systems following the methods described in Section 2.6. The four locations analyzed are identified in Figure 11. While each site features an 18-year-mean capacity factor similar to the mean across the island, one site on each side of the island features a high COV value, and the other a more typical value to serve as a control for our analysis. This is done to isolate the impact of high degrees of interannual variability.

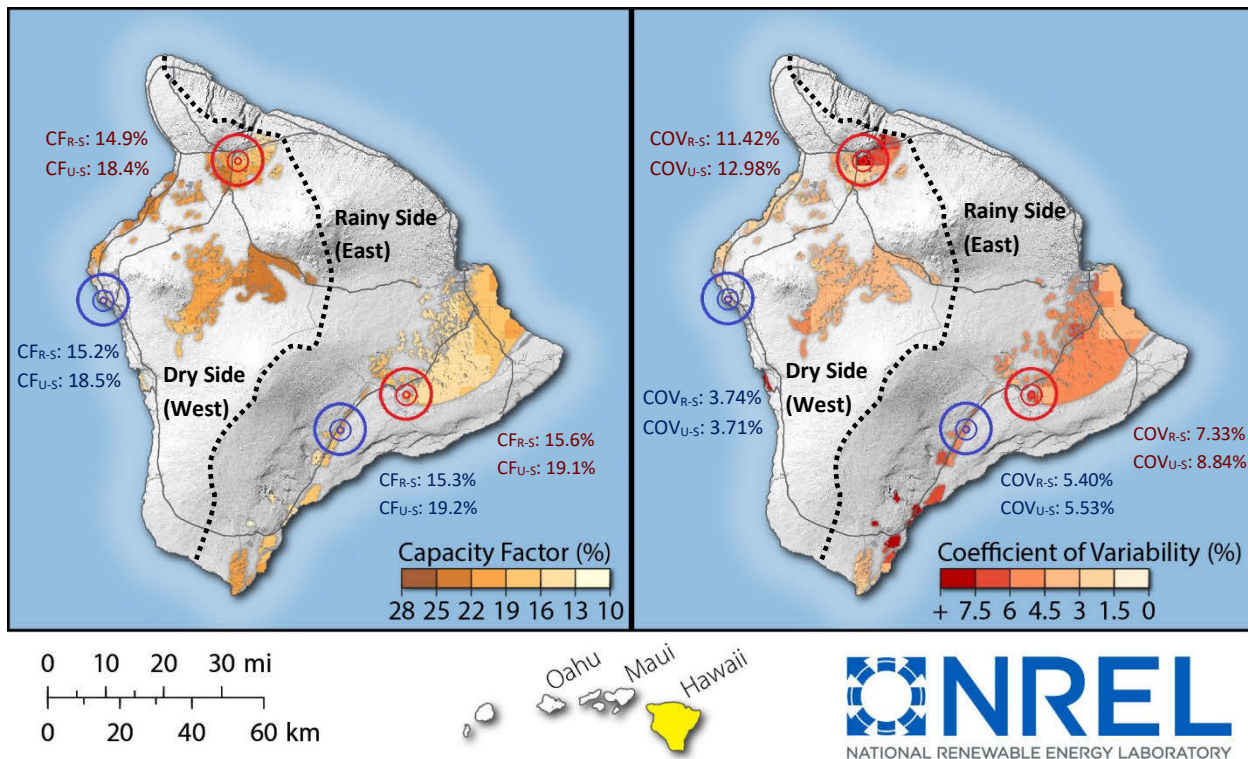




Figure 11: Two sites on either side of the Island of Hawaii with similar system capacity factors and very different coefficients of variability. The capacity factors and coefficients of variability of residential-scale (R-S) and utility-scale (U-S) photovoltaic systems are shown.

We compare the payback period and the NPV from the multiyear consideration to each of the single-year forward projections. Table 3 shows the tabulated results for the residential-scale system, and Table 4 shows the results for the utility-scale system. We then model the annual energy generation associated with the multiyear consideration and each of the single-year projections. Figure 12 and Figure 13 shows the results for sites on each side of the island for the residential-scale system, and Figure 14 and Figure 15 show the results for the utility-scale system.

Table 3: Payback periods and net present values of a residential-scale photovoltaic power system are calculated for each location assuming a multiyear consideration (1998–2015) data set at that location and assuming single-year forward projections of the lowest capacity factor year, the highest capacity factor year, and the typical meteorological time series. The single-year projections are compared to the multiyear consideration.

[Residential Scale: 30-Deg Roof Mounted, 5kW _{DC}]									
Zone	Coordinates	Planning Method	Data Set	CF	COV	Payback (years)	NPV (\$)	Consequence of Planning Method on Payback	Consequence of Planning Method on NPV
	19.33°N, 155.38°W	Multi-year Consideration	Full NSRDB (1998-2015)	15.3%	5.40%	5.87	\$8,572	Obtain True Value	Obtain True Value
	19.33°N, 155.38°W	Single-year Projection	Low CF Year (2014)	14.1%	n/a	7.52	\$6,452	1.7 year Over-Estimate	25% Under-Estimated
	19.33°N, 155.38°W	Single-year Projection	High CF Year (2000)	16.9%	n/a	5.66	\$9,585	0.2 year Under-Estimate	12% Over-Estimated
	19.33°N, 155.38°W	Single-year Projection	Single Sample (TMY)	15.3%	n/a	6.23	\$8,428	0.36 year Over-Estimate	2% Under-Estimated
	19.41°N, 155.26°W	Multi-year Consideration	Full NSRDB (1998-2015)	15.6%	7.33%	5.64	\$8,866	Obtain True Value	Obtain True Value
	19.41°N, 155.26°W	Single-year Projection	Low CF Year (2015)	14.0%	n/a	7.62	\$6,326	2.0 year Over-Estimate	29% Under-Estimated
	19.41°N, 155.26°W	Single-year Projection	High CF Year (2000)	17.1%	n/a	5.56	\$9,796	0.1 year Under-Estimate	10% Over-Estimated
	19.41°N, 155.26°W	Single-year Projection	Single Sample (TMY)	15.7%	n/a	6.09	\$8,692	0.5 year Over-Estimate	2% Under-Estimated
	19.69°N, 156.02°W	Multi-year Consideration	Full NSRDB (1998-2015)	15.2%	3.74%	6.40	\$8,262	Obtain True Value	Obtain True Value
	19.69°N, 156.02°W	Single-year Projection	Low CF Year (1998)	14.1%	n/a	6.85	\$7,382	0.4 year Over-Estimate	11% Under-Estimated
	19.69°N, 156.02°W	Single-year Projection	High CF Year (2009)	16.2%	n/a	6.25	\$8,394	0.2 year Under-Estimate	2% Over-Estimated
	19.69°N, 156.02°W	Single-year Projection	Single Sample (TMY)	15.0%	n/a	6.37	\$8,172	0.0 year Under-Estimate	1% Under-Estimated
	20.01°N, 155.66°W	Multi-year Consideration	Full NSRDB (1998-2015)	14.9%	11.42%	5.79	\$8,307	Obtain True Value	Obtain True Value
	20.01°N, 155.66°W	Single-year Projection	Low CF Year (2009)	12.4%	n/a	8.44	\$5,424	2.7 year Over-Estimate	35% Under-Estimated
	20.01°N, 155.66°W	Single-year Projection	High CF Year (2003)	16.9%	n/a	5.74	\$9,404	0.0 year Under-Estimate	13% Over-Estimated
	20.01°N, 155.66°W	Single-year Projection	Single Sample (TMY)	15.5%	n/a	6.17	\$8,533	0.4 year Over-Estimate	3% Over-Estimated

As shown in Table 3, for any location, if the single year selected for the economic decision-making features a low capacity factor, then the payback period will be overestimated. For one location on the west side of the Island of Hawaii, the payback period was inflated by more than 2.5 years. Further, selecting a year with a low capacity factor yields NPVs that grossly underestimate the true value of a potential PV project. In this case, a residential customer might conclude that the investment is not worthwhile. This translates into real-world lost economic opportunities from flawed assumptions about the solar resource and meteorological condition data sets that would be entirely hidden from the onset of the analysis.

Conversely, if the single year selected for the economic decision-making happens to feature a high capacity factor, then the payback period will be underestimated relative to the true values, albeit slightly. Further, this selection would yield NPVs that are inflated relative to the true values. Ultimately, this scenario would potentially result in residential customers opting to invest in PV, and the true economic benefit would be less than what was expected.

Of the single-year forward projections, the TMY data sets yield the most accurate payback periods and NPVs relative to the true values. The results still fail to reflect the consequences of interannual variability. As shown in Figure 12 and Figure 13, the annual power generated by such a system will deviate from that which was expected assuming a TMY data set. Therefore, during any given year, the true economic benefit of the PV system might be higher or lower than what might be expected if TMY data were used for the economic decision-making. This scenario might complicate the financial planning from a residential customer and might potentially delay or accelerate other investments.

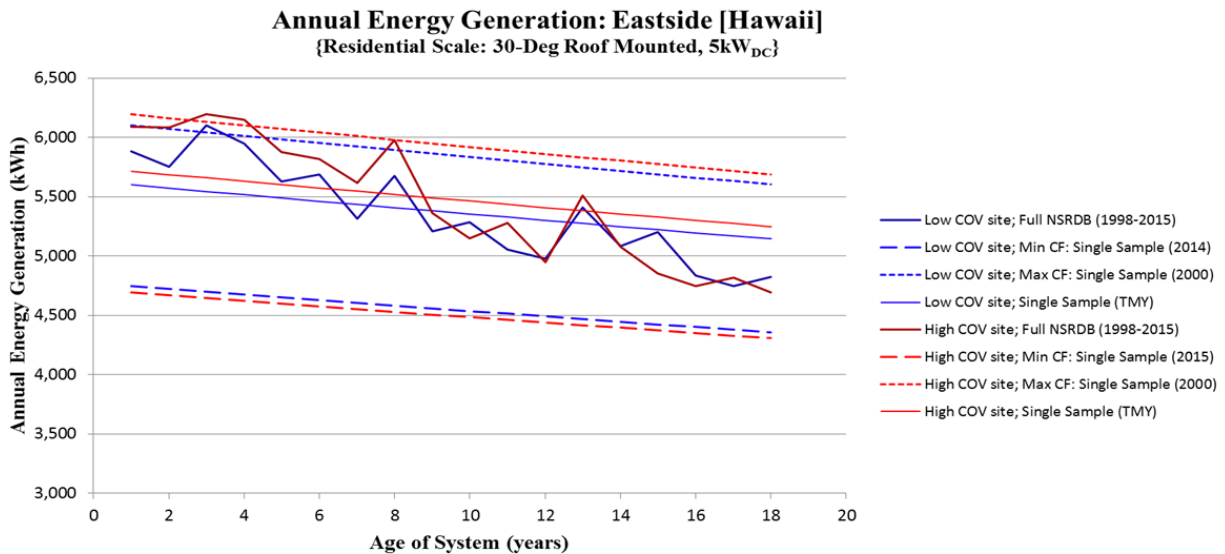


Figure 12: Annual energy generation of a residential-scale system assuming a multiyear consideration (1998–2015) at that location and assuming single-year forward projections of the lowest capacity factor year, the highest capacity factor year, and the typical meteorological year time series.

Annual Energy Generation: Westside [Hawaii] {Residential Scale: 30-Deg Roof Mounted, 5kW_{DC}}

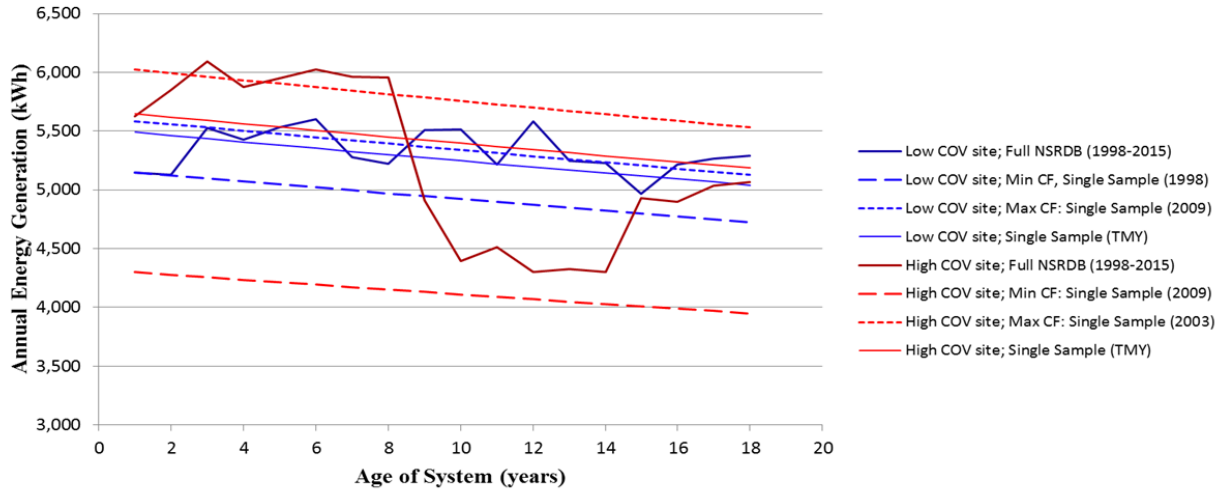


Figure 13: Annual energy generation of a residential-scale system assuming a multiyear consideration (1998–2015) at that location and assuming single-year projections of the lowest capacity factor year, the highest capacity factor year, and the typical meteorological year time series.

Table 4: Payback periods and net present values of a utility-scale photovoltaic power system are calculated for each location assuming a multiyear consideration (1998–2015) data set at that location and assuming single-year forward projections of the lowest capacity factor year, the highest capacity factor year, and the typical meteorological year time series. The single-year projections are compared to the multiyear consideration.

{Utility Scale: 1-Axis Tracking, 5MW_{DC}}

Zone	Coordinates	Planning Method	Data Set	CF	COV	Payback (years)	NPV (\$)	Consequence of Planning Method on Payback	Consequence of Planning Method on NPV
	19.33°N, 155.38°W	Multi-year Consideration	Full NSRDB (1998-2015)	19.2%	5.53%	3.19	\$5,715,911	Obtain True Value	Obtain True Value
	19.33°N, 155.38°W	Single-year Projection	Low CF Year (2014)	17.7%	n/a	3.89	\$4,321,985	0.7 year Over-Estimate	24% Under-Estimated
	19.33°N, 155.38°W	Single-year Projection	High CF Year (2000)	20.8%	n/a	3.16	\$6,279,101	0.0 year Under-Estimate	10% Over-Estimated
	19.33°N, 155.38°W	Single-year Projection	Single Sample (TMY)	19.2%	n/a	3.37	\$5,624,790	0.18 year Over-Estimate	2% Under-Estimated
	19.41°N, 155.26°W	Multi-year Consideration	Full NSRDB (1998-2015)	19.1%	8.84%	3.11	\$5,781,008	Obtain True Value	Obtain True Value
	19.41°N, 155.26°W	Single-year Projection	Low CF Year (2015)	16.7%	n/a	4.10	\$3,877,263	1.0 year Over-Estimate	33% Under-Estimated
	19.41°N, 155.26°W	Single-year Projection	High CF Year (2005)	21.4%	n/a	3.15	\$6,294,261	0.0 year Under-Estimate	9% Over-Estimated
	19.41°N, 155.26°W	Single-year Projection	Single Sample (TMY)	19.3%	n/a	3.36	\$5,654,542	0.3 year Over-Estimate	2% Under-Estimated
	19.69°N, 156.02°W	Multi-year Consideration	Full NSRDB (1998-2015)	18.5%	3.71%	3.62	\$5,244,567	Obtain True Value	Obtain True Value
	19.69°N, 156.02°W	Single-year Projection	Low CF Year (1998)	17.2%	n/a	3.71	\$4,727,668	0.1 year Over-Estimate	10% Under-Estimated
	19.69°N, 156.02°W	Single-year Projection	High CF Year (2009)	19.6%	n/a	3.47	\$5,345,925	0.2 year Under-Estimate	2% Over-Estimated
	19.69°N, 156.02°W	Single-year Projection	Single Sample (TMY)	18.2%	n/a	3.54	\$5,150,197	0.1 year Under-Estimate	2% Under-Estimated
	20.01°N, 155.66°W	Multi-year Consideration	Full NSRDB (1998-2015)	18.4%	12.98%	3.24	\$5,438,812	Obtain True Value	Obtain True Value
	20.01°N, 155.66°W	Single-year Projection	Low CF Year (2009)	14.7%	n/a	4.48	\$3,204,802	1.2 year Over-Estimate	41% Under-Estimated
	20.01°N, 155.66°W	Single-year Projection	High CF Year (2004)	21.2%	n/a	3.16	\$6,252,390	0.1 year Under-Estimate	15% Over-Estimated
	20.01°N, 155.66°W	Single-year Projection	Single Sample (TMY)	19.0%	n/a	3.39	\$5,557,440	0.2 year Over-Estimate	2% Over-Estimated

The most significant insight obtained from Table 4 is that any single-year forward projection for economic decision-making for a utility-scale system will deviate from the true economic value of the proposed PV system. More specifically, if a single year is selected that features a high capacity factor, then the NPV will be overestimated: 15% in one case for a location on the west side of the island. This discrepancy would translate to millions of dollars of overestimated value for a prospective utility-scale system. If a single projection was selected that features a low capacity factor, then the NPV will be grossly underestimated, which might kill a potential project and result in millions of dollars of lost opportunity. Even the TMY data set yields inaccurate economic metrics. The best course of action for making economic decisions is to avoid relying on single-year projections. Instead, any economic analysis should consider as much of the historical data as possible to capture the effects of interannual variability. Some level of uncertainty is associated with calculating the payback period and NPV of a PV system because of the interannual variability of the capacity factor at a given location. Our study should serve as a call to be aware of the interannual variability and to avoid relying on single-year forward projections without accounting for the interannual variability in economic decision-making for PV systems.

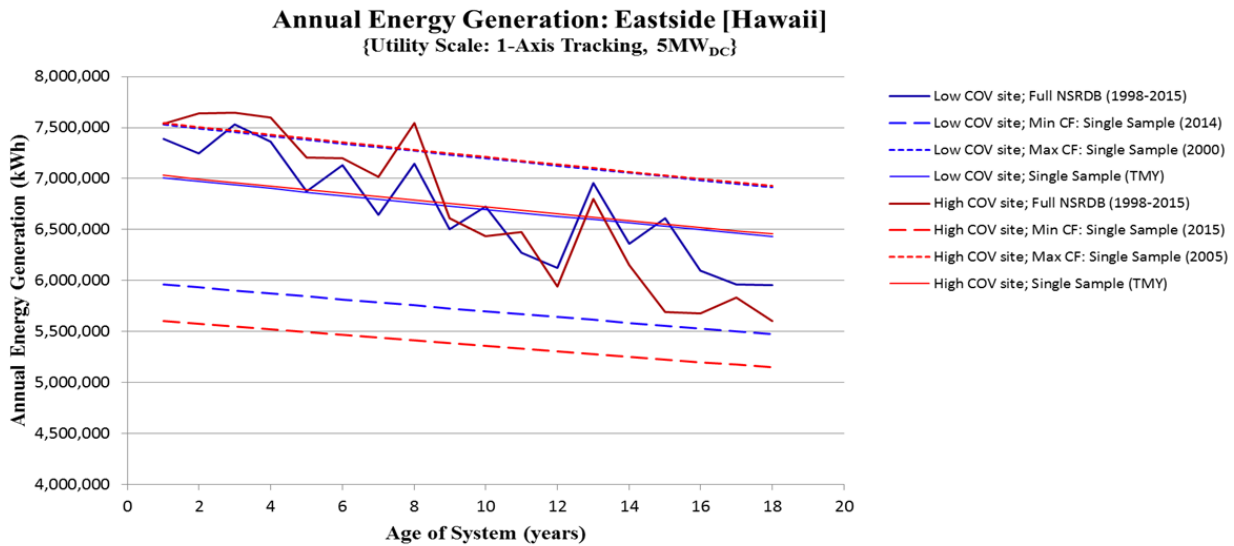


Figure 14: Annual energy generation of a utility-scale system assuming a multiyear consideration (1998–2015) at that location and assuming single-year projections of the lowest capacity factor year, the highest capacity factor year, and the typical meteorological year time series.

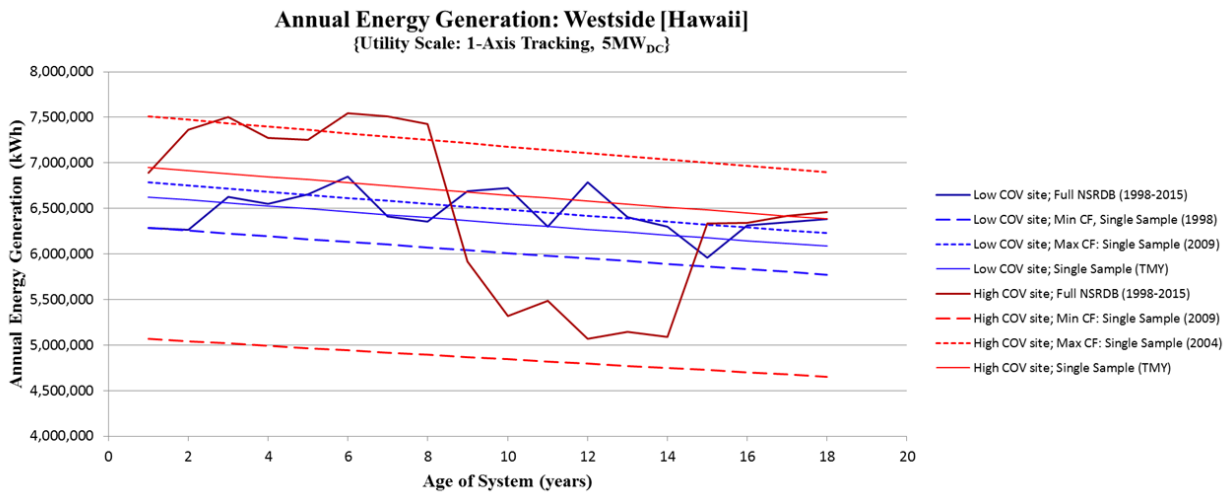


Figure 15: Annual energy generation of a utility-scale system assuming a multiyear consideration (1998–2015) at that location and assuming single-year projections of the lowest capacity factor year, the highest capacity factor year, and the typical meteorological year time series.

4 Conclusions

Regarding the solar resource in terms of GHI among the Hawaiian Islands, we identified significant interannual variability in both the annual mean values and monthly mean values. We spotted regular seasonal trends for GHI, atmospheric temperature, and PV system capacity factor across the Island of Hawaii. We noted that interannual variability is more pronounced during the late winter than during midsummer. Interestingly, sites and time periods that feature lower system capacity factors also feature more variability on an interannual basis. We found that the swings in capacity factor from one year to another can be significant.

We explored the distribution of capacity factors across each island for each of the 18 years considered. Surprisingly, the mean value and standard deviation of the distributions seem to vary by island. Each island hosts unique atmospheric conditions that impact the system capacity factor. The largest island features steep changes in elevation that might create zones where clouds form, explaining the increased overall variability and reduced mean capacity factor. In contrast, the relatively higher mean capacity factor and lower overall variability values among the smaller islands can be explained by considering that their climates more closely match nearby ocean climates, which have fewer clouds.

We found that the capacity factor and COV are inversely correlated; sites with a lower 18-year mean of capacity factor tend to exhibit more interannual variability in terms of COV and that this is true both with and without spatial exclusions across the Hawaiian Islands. We calculated a mean CF for a 0-degree tilt, 1-axis tracking 5MW PV system of 18.8% and a corresponding COV of 2.49% for the annual mean values across the Island of Hawaii, and a maximum COV of 10.95% for monthly values. The coefficient of variability seems to converge as more sample years are included in the analysis.

Regarding the economic planning of prospective residential and utility-scale PV systems, the payback period and NPV feature uncertainty because of the interannual variability of the solar resource in terms of irradiance and the ambient temperature at a given location. Additionally, the

economic discount rate, the loan interest rates, the value of energy inflation rate, and the PV system degradation rate contributes to the total uncertainty in the NPV. We leave quantifying the relative magnitude of the uncertainty introduced by each of these factors for future work. Further, the uncertainty is influenced by the order of the data set being relied upon; earlier years having a more significant impact because discounting, for example, would weigh early years more heavily. If the earliest years feature a large bias from the long-term average CF for a given location, then the resulting bias from the expected economic metrics would be larger. Furthermore, an economic assessment of the feasibility of a prospective PV system that relies on TMY data sets is suboptimal due to the interannual variability of the solar resource. The results of such an analysis will also likely be biased, albeit slightly, from reality. The economic bias error associated with a TMY data set is reduced significantly when the time horizon of the analysis spans many years. Still, the annual power generation of a PV system, and consequently the economic return, will deviate from what would be expected when projecting a TMY data set over a longer time horizon during any given year. Since the capacity factor might be higher or lower than expected during any given year, the economic bias error is far larger if the analysis considers only a single year of resource data rather than a TMY data set, or better still, a multiple year data set. It is best to accept that interannual variability exists and should be accounted for when evaluating the economics of a prospective PV system.

We focused on characterizing the interannual variability of the solar resource, and we studied its impact from the context of investments in PV systems. This represents only one of several situations when the interannual variability can have a profound impact, yet this phenomenon is often neglected. It can be illustrative to consider a situation when a battery is to be sized and paired with a renewable energy system, such as a PV system. Given that the power generated by the PV system will feature interannual variability, if a battery system were sized following an analysis that accounted for only 1 year of solar resource data, then it is possible that the battery capacity would be suboptimal during a multiyear consideration—as was similar for the NPV in this study. Therefore, the interannual variability of the solar resource and other meteorological variables should be thought of as broadly significant in any situation when a fixed investment or decision must be made based on the conclusions of an analysis of the solar resource or meteorological conditions. Accordingly, our results should serve as a call to be aware of what is often overlooked. The interannual variability of the solar resource and meteorological conditions should not be ignored.

Declarations of Interest: None

References

- Blair, N., Dobos, A.P., Freeman, J., Neises, T., Wagner, M., Ferguson, T., Gilman, P., Janzou, S., 2014. System advisor model, sam 2014.1. 14: General description. NREL Rep. No. TP-6A20-61019, Natl. Renew. Energy Lab. Golden, CO 13.
- Bryce, R., Losada Carreño, I., Kumler, A., Hodge, B., Roberts, B., Martinez-anido, B., 2018. Annually and monthly resolved solar irradiance and atmospheric temperature data across the Hawaiian archipelago from 1998-2015 with interannual summary statistics. *Data Br.* in press.
- Dobos, A.P., 2014. PVWatts Version 5 Manual. Golden, CO.
- Dubey, S., Sarvaiya, J.N., Seshadri, B., 2013. Temperature dependent photovoltaic (PV) efficiency and its effect on PV production in the world - A review. *Energy Procedia* 33, 311–321. <https://doi.org/10.1016/j.egypro.2013.05.072>
- Duffy, P.B., Bartlett, J., Dracup, J., Freedman, J., Madani, K., Waight, K., 2014. Final Project Report Climate Change Impacts on Generation of Wind, Solar, and Hydropower in California. Livermore, CA.
- Eerme, K., 2012. Interannual and Intraseasonal Variations of the Available Solar Radiation, in: Babatunde, E.B. (Ed.), *Solar Radiation*. InTech, Rijeka, Croatia, pp. 33–52.
- Elliott, D.L., Wendell, L.L., Gower, G.L., 1991. An Assessment of the Available Windy Land Area and Wind Energy Potential in the Contiguous United States. Pacific Northwest Lab.
- Fant, C., Adam Schlosser, C., Strzepek, K., 2015. The impact of climate change on wind and solar resources in southern Africa. *Appl. Energy* 161, 556–564. <https://doi.org/10.1016/j.apenergy.2015.03.042>
- Frazier, A.G., Giambelluca, T.W., Diaz, H.F., Needham, H.L., 2016. Comparison of geostatistical approaches to spatially interpolate month-year rainfall for the Hawaiian Islands. *Int. J. Climatol.* 36, 1459–1470. <https://doi.org/10.1002/joc.4437>
- Freeman, J., Whitmore, J., Kaffine, L., Blair, N., Dobos, A.P., 2013. System Advisor Model: Flat Plate Photovoltaic Performance Modeling Validation Report. Golden, CO.
- Frohlich, C., Lean, J., 1998. Total Solar Irradiance: Present Knowledge and Future Needs, in: *A Crossroads for European Solar & Heliospheric Physics*. pp. 239–242.
- Habte, A., Lopez, A., Sengupta, M., Wilcox, S., 2014. Temporal and Spatial Comparison of Gridded TMY, TDY, and TGY Data Sets, Technical Report TP-5D00-60886. Golden, CO.
- Habte, A., Sengupta, M., Lopez, A., 2017. Evaluation of the National Solar Radiation Database (NSRDB): 1998-2015, Technical Report TP-5D00-67722. Golden, CO.
- HECO, 2016. PSIPs Update Report: December 2016 Book 3 of 4, Docket No. 2014-0183.

- Hoogwijk, M., Faaij, A., Eickhout, B., de Vries, B., Turkenburg, W., 2005. Potential of biomass energy out to 2100, for four IPCC SRES land-use scenarios. *Biomass and Bioenergy* 29, 225–257. <https://doi.org/10.1016/J.BIOMBIOE.2005.05.002>
- Janjai, S., Deeyai, P., 2009. Comparison of methods for generating typical meteorological year using meteorological data from a tropical environment. *Appl. Energy* 86, 528–537. <https://doi.org/10.1016/j.apenergy.2008.08.008>
- Jerez, S., Tobin, I., Vautard, R., Montávez, J.P., López-Romero, J.M., Thais, F., Bartok, B., Christensen, O.B., Colette, A., Déqué, M., Nikulin, G., Kotlarski, S., Van Meijgaard, E., Teichmann, C., Wild, M., 2015. The impact of climate change on photovoltaic power generation in Europe. *Nat. Commun.* 6, 1–8. <https://doi.org/10.1038/ncomms10014>
- Jones, R.W., Renfrew, I.A., Orr, A., Webber, B.G.M., Holland, D.M., Lazzara, M.A., 2016. Evaluation of four global reanalysis products using in situ observations in the Amundsen Sea Embayment, Antarctica. *J. Geophys. Res. Atmos.* 121, 6240–6257. <https://doi.org/10.1002/2015JD024680>
- Karststadt, R., Dahle, D., Heimiller, D., Nealon, T., 2005. *Assessing the Potential for Renewable Energy on National Forest System Lands*. Golden, CO.
- Kopp, G., Lawrence, G., Rottman, G., 2005. The Total Irradiance Monitor (TIM): Science Results, in: *The Solar Radiation and Climate Experiment*. Springer New York, New York, NY, pp. 129–139. https://doi.org/10.1007/0-387-37625-9_8
- Lave, M., Kleissl, J., 2010. Solar variability of four sites across the state of Colorado. *Renew. Energy* 35, 2867–2873. <https://doi.org/10.1016/j.renene.2010.05.013>
- Perdigão, J., Salgado, R., Dasari, H., Costa, M.J., 2011. Inter Annual Variability of Surface Solar Radiation over Iberian Peninsula, in: *Proceedings of the Global Conference on Global Warming 2011*. Lisbon, Portugal, pp. 1–11.
- Perea, A., Honeyman, C., Kann, S., Mond, A., Shiao, M., Jones, J., Moskowicz, S., Smith, C., Gallagher, B., Rumery, S., Holm, A., O'Brien, K., Baca, J., 2016. *Solar Market Insight Report 2016 Year In Review | SEIA* [WWW Document]. URL <https://www.seia.org/research-resources/solar-market-insight-report-2016-year-review> (accessed 1.3.18).
- Perez, R., Burtis, L., Hoff, T., Swanson, S., Herig, C., 2004. Quantifying residential PV economics in the US—payback vs cash flow determination of fair energy value. *Sol. Energy* 77, 363–366. <https://doi.org/10.1016/J.SOLENER.2004.03.004>
- Pfeifroth, U., Mueller, R., 2012. Evaluation of Satellite-Based and Reanalysis Precipitation Data in the Tropical Pacific. *J. Appl. Meteorol. Climatol.* 52, 634–644. <https://doi.org/10.1175/JAMC-D-12-049.1>
- Pozo-Vázquez, D., Wilbert, S., Gueymard, C., Alados-Arboledas, L., Santos-Alamillos, F., Granados-Munoz, M., 2011. Interannual variability of long time series of DNI and GHI at PSA, Spain, in: *Proc SolarPACES Conf. Granada, Spain*, pp. 1–8.
- Rienecker, M.M., Suarez, M.J., Gelaro, R., Todling, R., Bacmeister, J., Liu, E., Bosilovich, M.G., Schubert, S.D., Takacs, L., Kim, G.K., Bloom, S., Chen, J., Collins, D., Conaty, A., Da Silva, A., Gu, W., Joiner, J., Koster, R.D., Lucchesi, R., Molod, A., Owens, T., Pawson, S., Pegion, P., Redder, C.R., Reichle, R., Robertson, F.R., Ruddick, A.G., Sienkiewicz, M., Woollen, J., 2011. MERRA: NASA's modern-era retrospective analysis for research and applications. *J. Clim.* 24, 3624–3648. <https://doi.org/10.1175/JCLI-D-11-00015.1>
- SEIA, 2017. *Solar Industry Data* [WWW Document]. URL <https://www.seia.org/solar-industry-data> (accessed 1.3.18).
- Short, W., Packey, D.J., Holt, T., 1995. *A manual for the economic evaluation of energy efficiency and renewable energy technologies*, NREL/TP-462-5173 A. Golden, CO. <https://doi.org/NREL/TP-462-5173>
- SolarPower Europe, 2017. *Global Market Outlook for Solar Power 2017-2021*. SolarPower Eur. 60 pgs.
- State of Hawaii, 2018. *Hawaii Clean Energy Initiative* [WWW Document]. URL <http://www.hawaii-cleanenergyinitiative.org/> (accessed 1.3.18).
- U.S. Energy Information Administration, 2016. *U.S. Energy Information Administration* [WWW Document]. URL <https://www.eia.gov/state/analysis.php?sid=HI> (accessed 8.11.17).
- Van Haaren, R., Fthenakis, V., 2011. GIS-based wind farm site selection using spatial multi-criteria analysis (SMCA): Evaluating the case for New York State. *Renew. Sustain. Energy Rev.* 15, 3332–3340. <https://doi.org/10.1016/J.RSER.2011.04.010>
- Vignola, F., Grover, C., Lemon, N., McMahan, A., 2012. Building a bankable solar radiation dataset. *Sol. Energy* 86, 2218–2229. <https://doi.org/10.1016/j.solener.2012.05.013>
- Viola, J.P., 2017. *2016 Renewable Portfolio Standard Status Report*. Honolulu, Hawai'i.
- Wies, R.W., Johnson, R. a., Agarwal, A.N., Chubb, T.J., 2004. Economic analysis and environmental impacts of a PV with diesel-battery system for remote villages. *IEEE Trans. Power Syst.* 20, 692–700. <https://doi.org/10.1109/PES.2004.1373209>
- Wilcox, S., Gueymard, C. a., 2010. Spatial and Temporal Variability of the Solar Resource in the United States. *Am. Sol. Energy Soc.* 1–8.

Yi, Y., Kimball, J.S., Jones, L.A., Reichle, R.H., McDonald, K.C., 2011. Evaluation of MERRA Land Surface Estimates in Preparation for the Soil Moisture Active Passive Mission. *J. Clim.* 24, 3797–3816. <https://doi.org/10.1175/2011JCLI4034.1>

Zakaria, Z.A., Bai-Chao, C., Hassan, M.O., 2008. Modeling of photovoltaic power plants, in: *International Conference Electrical Machines and Systems*, 2008. Wuhan, China, pp. 3835–3839.

Appendix A: Supplemental Figures

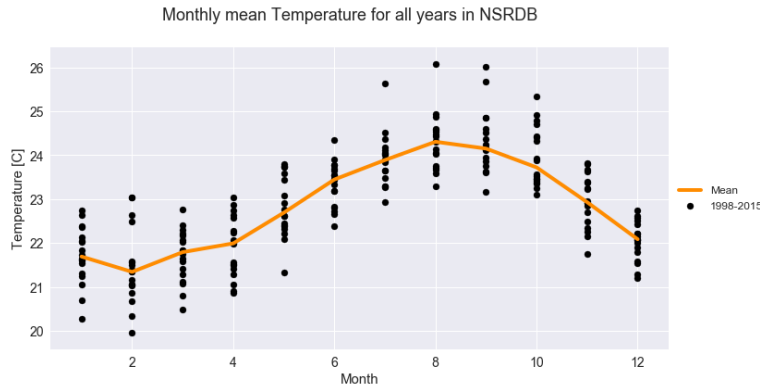


Figure A-1: Monthly mean temperature ($^{\circ}\text{C}$) across the Island of Hawaii for 1998–2015

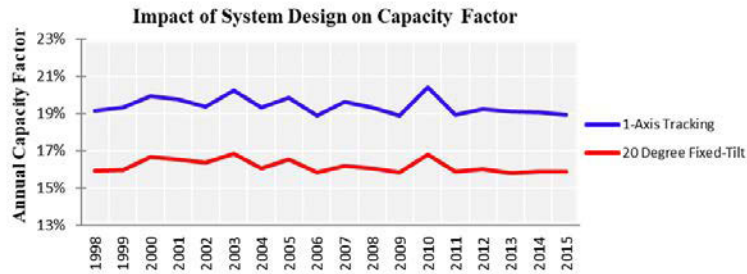


Figure A-2: Average annual capacity factor for utility-scale photovoltaic systems with two tracking configurations—1-axis tracking and 20-degree fixed tilt—across the Island of Hawaii.

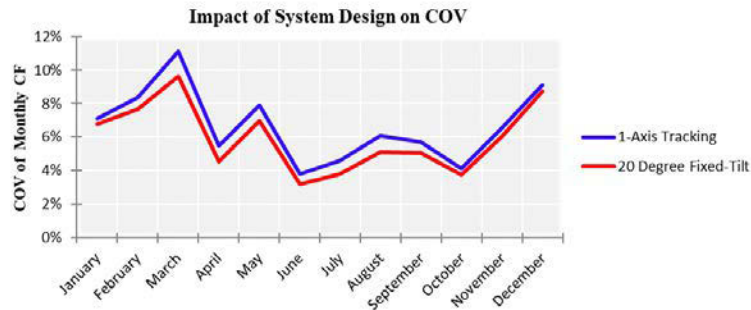


Figure A-3: Coefficient of variability of 18 years of monthly average capacity factor values across the Island of Hawaii.

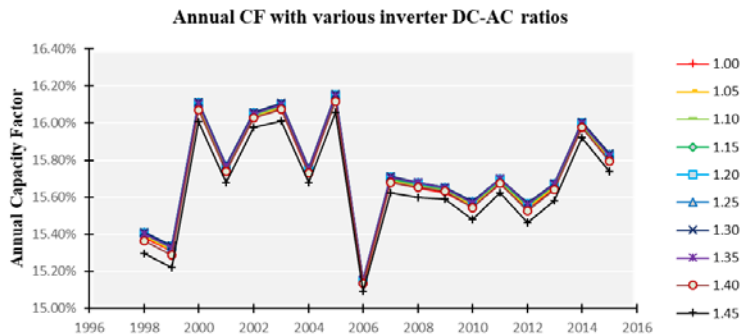


Figure A-4: Average annual capacity factor for all sites across the Island of Oahu for utility-scale photovoltaic systems with 20-degree fixed-tilt tracking and various DC-AC ratios.

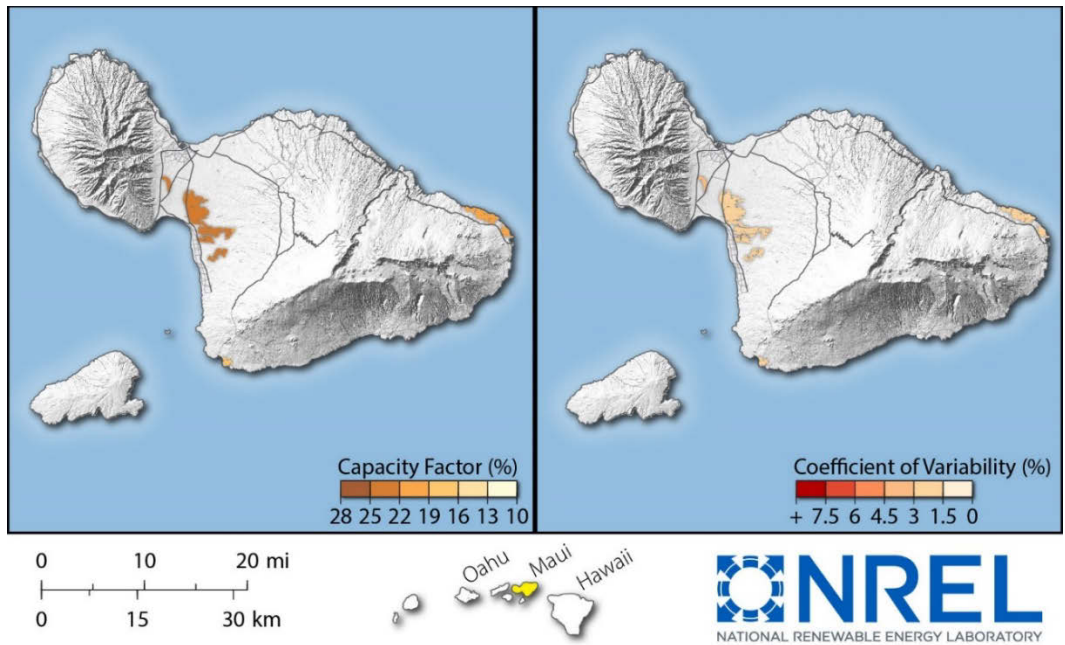


Figure A-5: (Left) The 18-year mean of capacity factor values of 1-axis tracking photovoltaic systems with tilt fixed at 0 degrees and an inverter DC-AC ratio of 1.2 for all zones suitable for constructing utility-scale photovoltaic systems across the Island of Maui. (Right) The coefficient of variability of annual capacity factor values for all the years contained in the NSRDB (1999–2015) of PV systems.

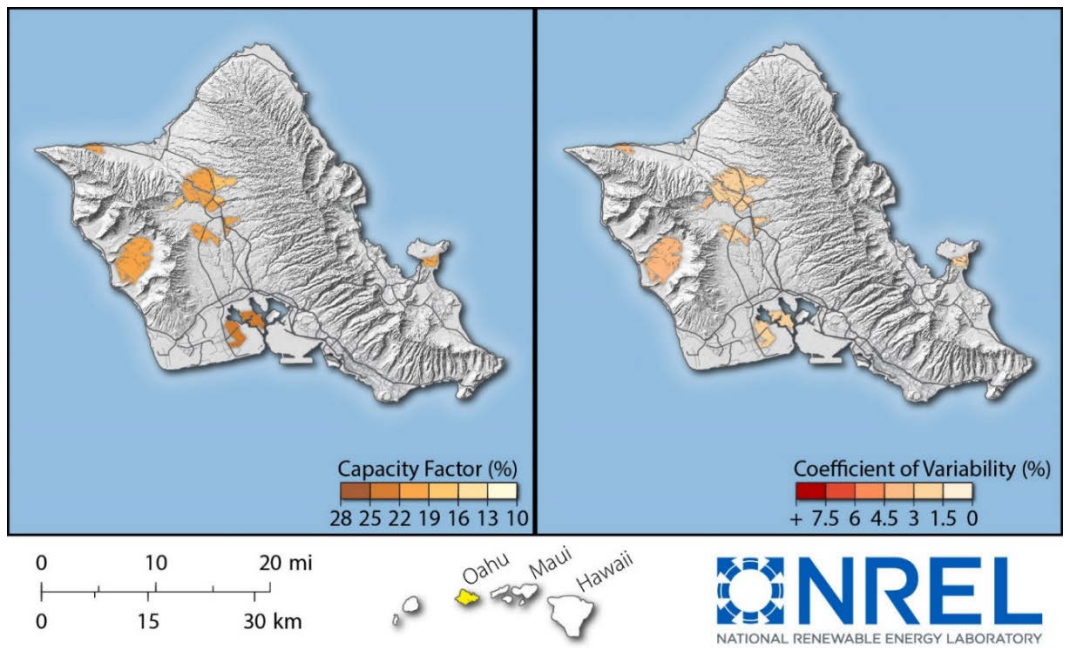


Figure A-6: (Left) The 18-year mean of capacity factor values of 1-axis tracking photovoltaic systems with tilt fixed at 0 degrees and an inverter DC-AC ratio of 1.2 for all zones suitable for constructing utility-scale photovoltaic systems across the Island of Oahu. (Right) The coefficient of variability of annual capacity factor values from 1999–2015

Summary Tables of Capacity Factor Values of PV Systems for Included Sites among the Hawaiian Islands (0-Deg. Tilt, 1-Axis Tracking, Inverter DC:AC Ratio of 1.2)

Month	1998	1999	2000	2001	2002	2003	2004	2005	2006	2007	2008	2009	2010	2011	2012	2013	2014	2015	Q1	Mean	Q3	Sdev	COV	Min	Max	Range		
Hawaii	January	18.2%	14.9%	15.7%	19.2%	15.0%	18.1%	16.1%	16.2%	15.6%	15.3%	16.8%	16.2%	17.7%	15.4%	17.2%	16.6%	16.2%	17.7%	15.6%	16.6%	17.6%	1.2%	7.40%	19.9%	19.2%	4.3%	
	February	19.5%	16.3%	21.2%	15.8%	18.1%	18.2%	17.5%	17.5%	16.3%	16.7%	16.7%	16.7%	18.9%	17.4%	17.7%	18.0%	16.7%	19.8%	16.7%	17.7%	18.3%	1.4%	8.02%	15.9%	21.2%	5.3%	
	March	20.4%	18.0%	19.8%	18.8%	19.7%	21.2%	16.0%	18.3%	12.9%	18.6%	19.3%	15.9%	19.1%	18.8%	17.4%	16.6%	17.3%	16.4%	16.8%	18.0%	19.2%	2.0%	10.95%	12.9%	21.2%	8.3%	
	April	18.6%	19.9%	20.1%	19.4%	15.8%	18.4%	19.3%	20.8%	19.1%	19.5%	16.6%	20.4%	18.7%	18.7%	20.5%	20.2%	20.0%	18.8%	19.5%	20.2%	18.8%	19.5%	2.0%	5.65%	16.6%	21.5%	4.9%
	May	17.9%	22.0%	20.8%	19.2%	23.7%	20.6%	23.2%	18.4%	22.1%	21.3%	19.9%	21.4%	19.0%	21.8%	19.5%	20.9%	19.1%	19.3%	20.6%	21.4%	1.6%	7.80%	17.9%	23.7%	5.8%		
	June	19.7%	22.5%	22.0%	20.8%	22.0%	22.0%	21.5%	21.0%	21.9%	22.2%	21.2%	21.0%	22.5%	20.6%	20.4%	21.8%	22.6%	21.0%	21.0%	21.5%	22.0%	0.8%	3.73%	19.7%	22.6%	2.9%	
	July	22.1%	23.3%	20.2%	22.4%	21.2%	21.8%	23.9%	21.9%	22.5%	23.4%	22.2%	20.6%	22.8%	22.4%	20.7%	21.2%	20.5%	21.9%	21.2%	22.0%	22.5%	1.0%	4.77%	20.2%	23.9%	3.7%	
	August	20.3%	20.6%	19.5%	23.2%	19.3%	21.1%	23.3%	21.6%	21.3%	24.4%	22.8%	21.0%	22.4%	20.9%	20.2%	22.5%	22.2%	18.9%	20.3%	21.2%	2.3%	1.3%	5.97%	18.9%	23.3%	4.4%	
	September	18.2%	19.9%	19.6%	20.3%	18.3%	20.9%	22.7%	19.0%	19.5%	18.7%	20.5%	19.5%	21.4%	19.5%	18.8%	21.7%	20.8%	18.2%	18.8%	19.9%	20.8%	1.3%	6.52%	18.2%	22.7%	4.5%	
	October	17.7%	18.0%	17.2%	17.6%	17.7%	19.1%	17.2%	17.5%	16.9%	18.7%	17.2%	18.1%	17.5%	17.8%	18.7%	16.6%	17.2%	18.3%	17.2%	17.7%	18.1%	0.7%	3.76%	16.6%	19.1%	2.5%	
	November	13.7%	14.8%	15.3%	15.4%	18.4%	15.0%	15.8%	16.5%	16.8%	15.4%	15.3%	15.0%	16.4%	13.9%	15.0%	14.0%	14.4%	15.0%	14.8%	15.3%	15.4%	1.1%	7.42%	13.7%	18.4%	4.7%	
	December	13.7%	14.3%	17.0%	15.4%	16.8%	14.8%	14.5%	16.4%	12.6%	13.2%	16.0%	14.7%	14.0%	14.3%	15.4%	16.1%	14.3%	15.1%	16.1%	14.4%	1.1%	8.99%	12.6%	17.4%	4.8%		
Annual Mean	18.3%	18.5%	19.1%	19.1%	18.8%	19.6%	19.1%	19.3%	18.1%	18.9%	18.9%	18.1%	19.6%	18.2%	18.4%	18.6%	18.7%	18.5%	18.4%	18.8%	19.1%	0.5%	2.49%	18.1%	19.6%	1.6%		
Kauai	January	18.0%	17.9%	18.7%	20.4%	16.5%	18.3%	17.1%	17.6%	19.2%	17.6%	18.6%	17.4%	18.7%	17.9%	19.0%	17.6%	18.4%	20.2%	17.6%	18.3%	18.7%	1.0%	5.48%	16.5%	20.4%	3.9%	
	February	21.6%	22.2%	22.1%	20.7%	21.0%	22.2%	18.9%	20.4%	20.4%	21.4%	20.3%	19.1%	19.9%	19.1%	21.5%	20.4%	18.8%	20.3%	19.7%	20.6%	21.5%	1.2%	5.69%	16.8%	22.5%	3.7%	
	March	24.3%	24.8%	24.0%	24.1%	24.1%	23.5%	20.4%	21.6%	16.7%	22.1%	24.5%	20.4%	23.3%	23.4%	20.7%	21.0%	21.5%	21.0%	21.1%	22.3%	24.1%	2.1%	9.30%	16.7%	24.8%	8.2%	
	April	24.8%	26.4%	26.2%	26.2%	24.5%	24.8%	25.8%	26.8%	25.2%	26.2%	24.0%	21.2%	25.2%	25.0%	25.8%	26.4%	25.1%	24.5%	24.8%	25.3%	26.2%	1.1%	4.45%	22.1%	26.8%	4.7%	
	May	23.8%	28.1%	28.2%	26.6%	24.6%	27.9%	26.1%	27.4%	26.2%	27.5%	27.1%	25.1%	28.3%	25.5%	28.3%	25.7%	26.3%	25.1%	25.5%	26.5%	27.8%	1.4%	5.62%	23.8%	28.3%	4.5%	
	June	25.4%	27.6%	27.8%	25.8%	27.6%	24.1%	27.7%	28.1%	28.0%	26.6%	25.6%	29.9%	26.7%	25.3%	25.3%	26.6%	26.9%	25.5%	25.5%	26.7%	27.8%	1.4%	5.09%	24.1%	29.5%	5.4%	
	July	26.4%	25.9%	28.2%	24.5%	24.3%	23.2%	29.0%	25.9%	25.9%	23.9%	26.9%	25.7%	24.3%	24.4%	26.7%	27.2%	25.8%	24.3%	24.3%	25.7%	26.4%	1.5%	5.85%	23.2%	29.0%	5.8%	
	August	26.1%	26.8%	25.7%	25.9%	23.9%	26.4%	25.9%	27.7%	25.7%	26.4%	24.3%	24.7%	23.1%	26.0%	26.8%	26.3%	26.3%	24.9%	25.6%	26.3%	25.5%	1.5%	5.68%	22.6%	28.3%	5.8%	
	September	23.4%	25.7%	24.5%	22.7%	23.7%	25.2%	23.8%	23.9%	22.8%	22.4%	22.1%	24.4%	22.0%	23.2%	23.1%	24.7%	23.1%	22.7%	22.7%	23.5%	24.3%	1.1%	4.48%	22.0%	25.7%	3.7%	
	October	19.9%	20.0%	21.0%	21.7%	20.5%	20.8%	20.5%	21.2%	19.9%	20.5%	21.1%	20.2%	21.1%	20.2%	21.1%	19.9%	20.4%	21.1%	20.0%	20.5%	21.1%	0.7%	3.63%	19.1%	21.7%	2.6%	
	November	15.3%	16.5%	19.2%	17.7%	18.0%	19.5%	18.5%	17.8%	17.6%	18.1%	17.4%	16.8%	18.3%	16.7%	17.0%	16.6%	18.3%	17.0%	16.9%	17.6%	18.2%	1.0%	5.83%	15.3%	19.5%	4.2%	
	December	16.5%	15.9%	18.5%	17.9%	19.3%	15.9%	16.8%	18.3%	16.7%	14.3%	14.9%	19.7%	16.0%	16.5%	16.4%	17.0%	15.5%	17.9%	15.9%	16.9%	17.9%	1.5%	8.67%	14.3%	19.7%	5.4%	
Annual Mean	22.1%	23.2%	23.7%	22.9%	22.3%	22.6%	22.6%	23.1%	22.0%	22.2%	22.1%	22.2%	22.4%	21.7%	22.6%	22.6%	22.1%	22.0%	22.1%	22.5%	22.6%	0.5%	2.19%	21.7%	23.7%	2.0%		
Maui	January	16.6%	13.9%	13.6%	16.7%	13.8%	15.7%	16.4%	14.8%	13.5%	13.9%	14.3%	14.8%	15.7%	15.2%	15.4%	14.0%	16.0%	17.1%	13.9%	15.1%	15.9%	1.2%	7.84%	13.5%	17.1%	3.6%	
	February	18.4%	15.6%	18.8%	15.4%	16.8%	17.2%	16.7%	15.6%	13.2%	16.0%	17.2%	16.1%	18.4%	14.8%	15.0%	17.4%	13.2%	19.2%	15.4%	16.4%	17.4%	1.7%	10.68%	13.2%	19.2%	6.1%	
	March	20.9%	18.6%	21.1%	20.5%	17.0%	19.6%	17.3%	18.5%	12.1%	18.2%	20.2%	16.9%	17.2%	18.8%	18.0%	16.9%	17.7%	17.7%	17.2%	18.2%	19.4%	2.1%	11.38%	12.1%	21.1%	9.1%	
	April	19.2%	21.7%	19.4%	19.1%	22.1%	21.1%	19.7%	21.6%	18.9%	22.9%	21.2%	18.1%	19.4%	20.9%	20.2%	20.2%	20.8%	22.6%	19.4%	20.5%	21.5%	1.4%	6.68%	18.1%	22.9%	4.8%	
	May	19.1%	21.2%	25.7%	24.0%	19.4%	22.7%	22.4%	25.2%	21.7%	24.4%	24.3%	23.7%	22.2%	19.8%	24.9%	23.8%	21.3%	23.9%	21.4%	22.8%	24.2%	2.0%	8.80%	19.1%	25.7%	6.6%	
	June	20.4%	23.3%	25.6%	23.0%	24.8%	25.2%	23.4%	24.7%	24.4%	23.9%	25.4%	22.0%	24.2%	25.0%	25.4%	26.0%	26.0%	23.3%	24.3%	25.2%	1.7%	6.99%	20.4%	28.0%	7.6%		
	July	23.9%	22.1%	22.7%	24.6%	23.1%	25.6%	27.3%	23.1%	23.9%	23.5%	25.4%	22.4%	23.2%	24.0%	23.2%	25.4%	25.0%	26.4%	23.1%	24.2%	25.3%	1.5%	6.23%	22.1%	27.3%	5.2%	
	August	22.9%	23.0%	22.3%	21.1%	21.1%	24.1%	22.7%	25.9%	22.4%	23.9%	23.6%	21.4%	22.6%	22.6%	22.6%	25.0%	25.8%	25.4%	23.9%	22.5%	23.4%	1.5%	6.36%	21.1%	25.9%	4.7%	
	September	22.3%	21.7%	19.4%	21.3%	21.0%	22.7%	22.5%	21.0%	21.2%	23.2%	22.7%	22.0%	21.9%	22.9%	22.2%	21.8%	23.9%	20.9%	21.2%	21.8%	22.5%	1.3%	4.87%	19.4%	23.9%	4.6%	
	October	18.3%	17.0%	18.3%	16.4%	17.1%	18.2%	17.7%	16.1%	17.3%	16.4%	17.0%	19.3%	17.4%	20.0%	18.5%	17.8%	19.4%	17.0%	17.7%	18.4%	11.1%	1.8%	11.4%	17.8%	20.0%	3.9%	
	November	14.1%	14.6%	16.1%	15.2%	15.2%	15.6%	14.0%	15.2%	15.9%	15.5%	14.0%	14.4%	14.7%	14.6%	15.9%	14.6%	15.8%	13.8%	14.4%	14.9%	15.6%	0.7%	5.00%	13.8%	16.1%	2.3%	
	December	12.4%	11.9%	15.1%	14.2%	14.7%	12.9%	11.2%	17.1%	14.0%	11.9%	11.8%	16.3%	12.3%	14.9%	12.6%	14.5%	14.2%	16.0%	12.3%	13.8%	15.1%	1.8%	12.83%	11.2%	17.1%	5.9%	
Annual Mean	19.0%	18.7%	19.9%	19.3%	18.8%	20.0%	19.3%	19.9%	18.1%	19.4%	19.6%	19.0%	19.4%	19.1%	19.8%	20.0%	19.9%	20.7%	19.1%	19.4%	19.9%	0.6%	3.06%	18.1%	20.7%	2.6%		
Niihau	January	17.1%	17.4%	18.8%	17.9%	16.2%	16.4%	15.9%	15.7%	17.3%	15.9%	18.6%	17.0%	17.1%	17.1%	16.2%	16.3%	17.3%	18.9%	16.3%	17.0%	17.4%	1.0%	5.93%	15.5%	18.9%	3.4%	
	February	20.7%	20.0%	20.5%	19.3%	22.0%	22.0%	17.1%	20.0%	19.0%	19.7%	18.5%	19.8%	20.3%	17.0%	18.7%	21.1%	16.8%	18.7%	18.7%	19.5%	20.4%	1.6%	7.96%	16.8%	22.0%	5.3%	
	March	22.3%	22.7%	22.3%	21.4%	23.2%	21.0%	19.2%	21.8%	13.9%	19.4%	21.3%	19.2%	22.8%	21.0%	20.6%	19.3%	21.6%	20.7%	19.7%	20.8%	22.2%	2.1%	10.22%	13.9%	23.2%	9.2%	
	April	24.2%	23.7%	24.1%	23.7%	22.1%	24.0%	24.7%	25.0%	24.9%	25.1%	21.7%	21.0%	22.8%	21.3%	23.2%	22.2%	24.5%	25.2%	22.4%	23.5%	24.6%	1.4%	5.77%	21.0%	25.2%	4.2%	
	May	23.7%	22.4%	24.5%	24.7%	21.7%	25.7%	25.0%	25.5%	26.3%	23.0%	24.3%	22.0%	22.6%	22.1%	21.7%	23.3%	22.1%	21.7%	25.3%	22.5%	23.9%	2.6%	1.6%	6.83%	21.7%	26.3	